

Phosphorus–Nitrogen Compounds. Part 24. Syntheses, Crystal Structures, Spectroscopic and Stereogenic Properties, Biological Activities, and DNA Interactions of Novel Spiro-ansa-spiro- and Ansa-spiro-ansa-cyclotetraphosphazenes

Gamze Elmas (nee Egemen),[†] Aytuğ Okumuş,[†] Zeynel Kılıç,^{*,†} Tuncer Hökelek,[‡] Leyla Açıık,[§] Hakan Dal,[⊥] Nagehan Ramazanoglu,[§] and L.Yasemin Koç[#]

[†]Department of Chemistry, Ankara University, 06100 Ankara, Turkey

[‡]Department of Physics, Hacettepe University, 06800 Ankara, Turkey

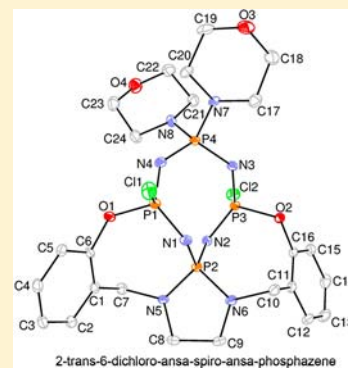
[§]Department of Biology, Gazi University, 06500 Ankara, Turkey

[⊥]Department of Chemistry, Anadolu University, 26470 Eskişehir, Turkey

[#]Department of Biology, Ankara University, 06100 Ankara, Turkey

Supporting Information

ABSTRACT: The reactions of octachlorocyclotetraphosphazene, $N_4P_4Cl_8$, with N_2O_2 donor-type aminopodands (**1a**, **1b**, **1g**, and **1h**) afforded two kinds of derivatives, namely, spiro-ansa-spiro (**sas**) (**2a**, **2b**, **2g**, and **2h**) and ansa-spiro-ansa (**asa**) (**3a** and **3b**) phosphazenes. The partly substituted **sas** phosphazenes (**2a** and **2b**) reacted with excess pyrrolidine and morpholine in tetrahydrofuran to produce the tetrapyrrolidino (**2c** and **2d**) and morpholino (**2e** and **2f**) derivatives. The reactions of the **asa** phosphazenes (**3a** and **3b**) with excess pyrrolidine and morpholine produced *gem*-2-*trans*-6-dichloropyrrolidinophosphazenes (**3c** and **3d**) and -morpholinophosphazenes (**3e** and **3f**). However, the fully substituted products were not obtained in these solvents. In addition, the expected fully substituted compound was not obtained from the reaction of **3a** with excess pyrrolidine by standard or microwave-assisted methods. The reaction of the long-chain starting compound (**1g**) with $N_4P_4Cl_8$ gave **sas** (**2g**) and the interesting 2,6-ansa-spiro-bicyclo product (**bicyclo-2,6-as**; **4g**), while the reaction of **1h** with $N_4P_4Cl_8$ yielded only **sas** (**2h**). The structural investigations of the compounds were verified by elemental analyses, mass spectrometry, Fourier transform infrared, and DEPT, HSQC, HMBC, 1H , ^{13}C , and ^{31}P NMR techniques. The crystal structures of **2b**, **3a**, **3b**, **3e**, and **4g** were determined by X-ray crystallography. Compounds **2a–2h**, **3a–3f**, and **4g** had two stereogenic P atoms. Compound **3b** had one enantiomer according to the Flack parameter, and **3f** was a racemic mixture, as shown by chiral high-performance liquid chromatography and chiral-solvating-agent, (*R*)-(+)-2,2,2-trifluoro-1-(9'-anthryl)ethanol, experiments. Furthermore, compounds **2a**, **2c**, and **2d** exhibited weak antibacterial activity against (*G*+) bacterium, and **3c** and **3d** displayed moderate antifungal activity against *Candida tropicalis*. Gel electrophoresis data demonstrated that **2e**, **3c**, and **3e** promoted the formation of DNA cleavage. The prevention of *Bam*HI digestion by **2a–2f** and **3a–3f**, except **2b** and **2e**, disclosed binding with GG nucleotides in DNA.



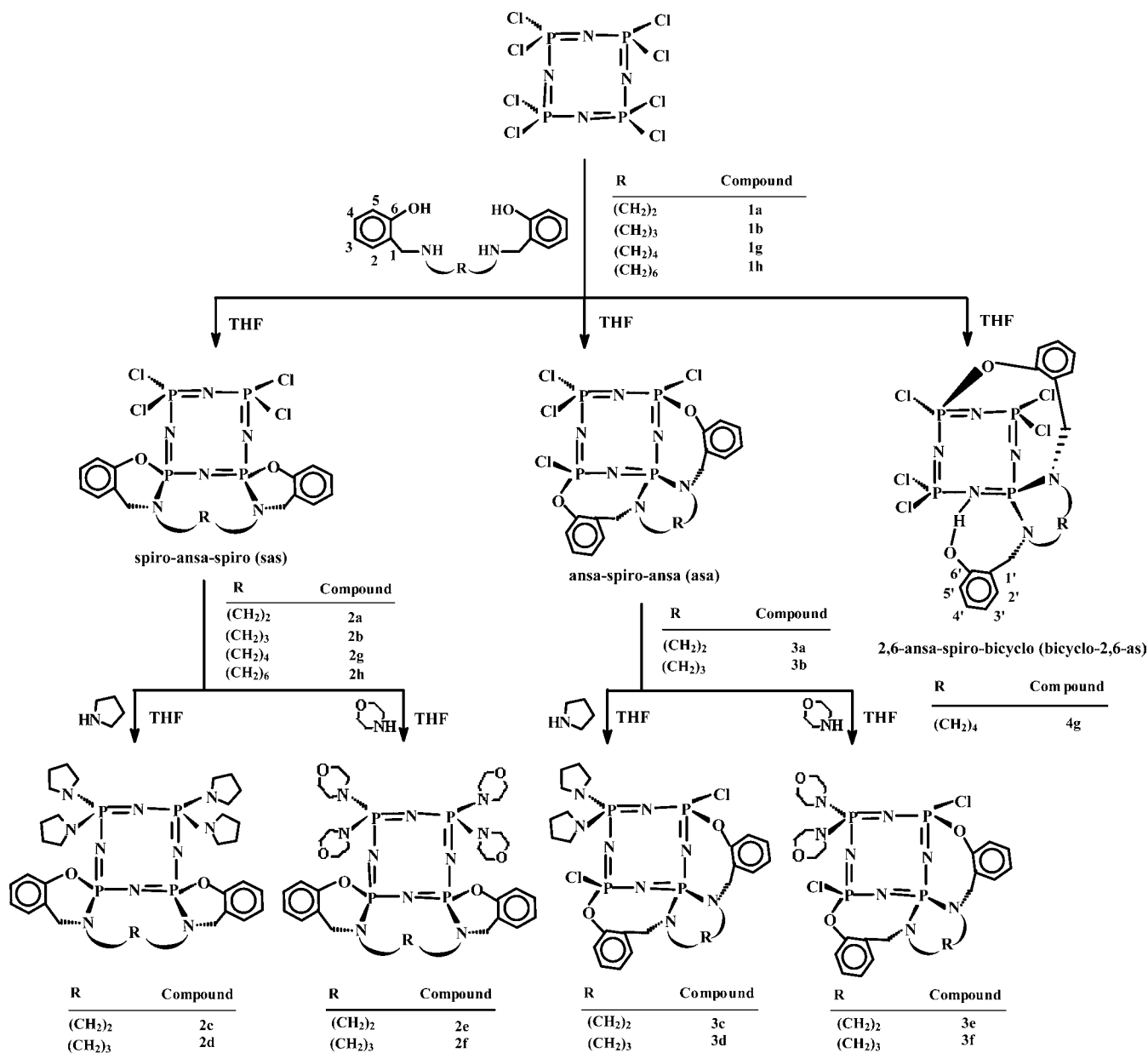
INTRODUCTION

Cyclophosphazenes are an important class of inorganic ring systems and exhibit very different physical and chemical properties depending on the types and properties of the substituents bonded to the P atoms.¹ The replacement reaction patterns of Cl atoms in $N_3P_3Cl_6$ with mono-, di-, tri-, and tetrafunctional amines, such as diaminoalkanes, diaminopolyethers, spermidine, and spermine, have been extensively studied² and reported as chemotherapeutic agents and selective carriers for delivering anticancer drugs to malignant target cells.³ Although a large number of $N_4P_4Cl_8$ derivatives have also been prepared with mono- and difunctional ligands,⁴ discussions of the substitution reaction patterns with polyfunctional ligands are relatively limited in the literature.⁵ $N_4P_4Cl_8$ with bidentate and/or polydentate amines may produce spiro,

dispiro (2,4- and 2,6-), trispiro, tetraspiro, ansa, spiro-ansa (2,4- and 2,6-), spiro-ansa-spiro (**sas**), bino, spiro-bino, and di(spiro-bino) products depending on the reaction conditions.⁶ Our group has focused on the reactions of N_2O_2 donor-type tetradentate ligands with $N_3P_3Cl_6$ and isolated **sas** and spiro-bino-spiro (**sbs**) but not ansa-spiro-ansa (**asa**) products.⁷ A review of the literature shows that there are no reports of the reactions of $N_4P_4Cl_8$ with N_2O_2 donor-type tetradentate ligands. This paper is focused primarily on the chloride replacement reactions of $N_4P_4Cl_8$ with N_2O_2 tetradentate ligands with the aim of obtaining novel polyheterocyclotetraphosphazenes for comparison with cyclotriphosphazene

Received: August 7, 2012

Published: November 19, 2012

Scheme 1. Phosphazene Derivatives Obtained from the Reactions of $N_4P_4Cl_8$ with Aminopodands, Pyrrolidine, and Morpholine

derivatives and also exploring their biological activity. The stereogenic properties of cyclo-triphosphazene derivatives are a new subject of interest.⁸ The stereogenic properties of some of the cyclo-triphosphazene derivatives have been investigated using ^{31}P NMR spectroscopy in the presence of chiral-solvating-agent (CSA) and high-performance liquid chromatography (HPLC) techniques.⁹ Cyclo-triphosphazenes have been extensively used as building blocks for the synthesis of phosphazenes, polymers, and dendrimers, and cyclophosphazenes may be useful as strong bases in the syntheses of coordination complexes. Chiral cyclophosphazenes are important compounds for the preparation of chiral complexes and polymers.¹⁰ Organophosphazenes have various applications of technological and medicinal importance, such as the production of inflammable textile fibers,¹¹ hydraulic fluids,¹² lubricants,¹³ ionic liquids,¹⁴ liquid-crystalline materials,¹⁵ advanced elastomers,¹⁶ rechargeable lithium batteries,¹⁷ anticancer and antimicrobial agents,¹⁸ membranes,¹⁹ and synthetic bones and

biomedical materials.^{20,21} Octapyrrolidinocyclo-tetraphosphazene has significant anticancer activity.²² The copper(II) complex of a fully phenoxy-substituted star-branched cyclo-tetraphosphazene derivative is active in the oxidative cleavage of DNA.²³

The choice of tetradentate symmetric ligands is very important for this study because stereochemically controlled reactions can be achieved with these ligands, leading to the arrangement of configurations of tetracoordinated P and tricoordinated N atoms, which form stereogenic centers. If the N atoms have three different substituents and restricted single-bond rotations about N atoms, atropisomerism may arise in cyclo-tetraphosphazene derivatives. This phenomenon is well-known for some organic compounds.²⁴

We report herein (i) the synthesis of novel sas (2a–2h), asa (3a–3f), and 2,6-ansa-spiro-bicyclo (bicyclo-2,6-as; 4g) cyclo-tetraphosphazenes with conventional methods and microwave-assisted preparations of 3c (Scheme 1), (ii) the structural

determination of compounds by mass spectrometry (MS), Fourier transform infrared (FTIR), one-dimensional (1D) ^1H , ^{13}C , and ^{31}P NMR, distortionless enhancement by polarization transfer (DEPT), and two-dimensional (2D) heteronuclear single quantum coherence (HSQC), and heteronuclear multiple-bond correlation (HMBC) techniques, (iii) the solid-state and molecular structures of **2b**, **3a**, **3b**, **3e**, and **4g**, (iv) the stereogenic properties of **3f** investigated by ^{31}P NMR measurements in the presence of CSA and chiral HPLC, (v) the investigations of antibacterial and antifungal activities of **2a–2f** and **3a–3f**, and (vi) interactions between the compounds **2a–2f**, **3a–3f**, and pBR322 DNA.

EXPERIMENTAL SECTION

General Methods. Commercial-grade reagents were used without further purification. Solvents were dried and distilled by standard methods. All reactions were monitored using thin-layer chromatography (TLC) on Merck DC Alufolien Kiesegel 60 B₂₅₄ sheets. Column chromatography was performed on Merck Kiesegel 60 (230–400 mesh ATSM) silica gel. All reactions were carried out under an argon atmosphere. Melting points were measured on a Gallenkamp apparatus using a capillary tube. ^1H , ^{13}C , and ^{31}P NMR, HSQC, DEPT, and HMBC spectra were recorded on a Bruker DPX FT-NMR (500 MHz) spectrometer (SiMe₄ as internal and 85% H₃PO₄ as external standards). The spectrometer was equipped with a 5 mm PABBO BB inverse-gradient probe. Standard Bruker pulse programs²⁵ were used. The numbering of the protons and carbons of all of the phosphazene derivatives is given in Scheme 1. IR spectra were recorded on a Mattson 1000 FTIR spectrometer in KBr disks and were reported in cm⁻¹ units. Microanalyses were carried out by the microanalytical service of TUBITAK Turkey. APIES-MS spectra were recorded on an Agilent 1100 MSD spectrometer. Microwave-assisted experiments have been performed with a Milestone Start S system by using a weflon magnet for tetrahydrofuran (THF), toluene, and *o*-xylene. Experiments involving the CSA were carried out by the addition of small aliquots of a concentrated solution of CSA in the solvent used for NMR spectroscopy and the proton-decoupled ^{31}P NMR spectrum recorded at each addition. HPLC experiments were performed with an Agilent 1100 series HPLC system (Chemstation software) equipped with a G 1311A pump and a G 1315B diode-array detector monitoring the range of 220–360 nm. The detection wavelength was set at 254 nm for **3f**. A reversible chiral column (R,R)-whelk-01 (250 × 4.6 mm) from Regis Tech. Inc. was used for HPLC. Antibacterial susceptibility testing was performed by the BACTEC MGIT 960 (Becton Dickinson, Sparks, MD) system using the agar-well diffusion method²⁶ (section S1 in the Supporting Information, SI). The DNA binding abilities were examined using agarose gel electrophoresis (section S2 in the SI).^{27,28}

The starting compounds N₄P₄Cl₈ (a gift from Otsuka Chemical Co. Ltd.), aliphatic amines (Fluka), pyrrolidine (Fluka), morpholine (Fluka), and salicylaldehyde (Fluka) were purchased. The CSA was obtained from Aldrich Chemical Co.

Preparation of Compounds. 2,2'-[1,2-Ethanediyldis-(iminomethanediyl)]diphenol (**1a**), 2,2'-[1,3-propanediyldis-(iminomethanediyl)]diphenol (**1b**), 2,2'-[1,4-butanediyldis-(iminomethanediyl)]diphenol (**1g**), and 2,2'-[1,6-hexanediyldis-(iminomethanediyl)]diphenol (**1h**) have been synthesized according to the methods reported in the literature.²⁹

sas 2a and asa 3a. K₂CO₃ (3.00 g, 22.00 mmol) was added to a stirred solution of **1a** (1.50 g, 5.50 mmol) in dry THF (200 mL). The mixture was refluxed for 4 h and cooled to ambient temperature. Afterward, a mixture of triethylamine (6.10 mL) and N₄P₄Cl₈ (2.55 g, 5.50 mmol) in dry THF (100 mL) is added dropwise to the stirred solution of **1a** at -10 °C for over 5 h. After the mixture had been allowed to warm to ambient temperature, it was stirred for 16 h under an argon atmosphere. The precipitated amine hydrochloride and excess K₂CO₃ were filtered off, and the solvent was evaporated. The

products, **2a** and **3a**, were purified by column chromatography with toluene.

Compound **2a** was crystallized from acetonitrile. Yield: 0.36 g (22%). Mp: 249 °C. Anal. Calcd for C₁₆H₁₆O₂N₆P₄Cl₄: C, 32.57; H, 2.73; N, 14.24. Found: C, 32.76; H, 2.77; N, 14.28. APIES-MS (fragments are based on ³⁵Cl; Ir % designates the fragment abundance percentage): *m/z* 589 ([MH]⁺, 87). FTIR (KBr, cm⁻¹): ν 3067 (asymm), 3027 (symm, C–H arom), 2920, 2851 (C–H aliph), 1579 (C=C), 1313 (asymm), 1180 (symm, P=N), 544 (asymm), 483 (symm, PCl). ^1H NMR (500 MHz, CDCl₃, ppm): δ 7.26 (m, 2H, H₄), 7.07 (m, 6H, H₂, H₃, H₅), 4.62 (dd, 2H, $^2J_{\text{HH}} = 11.5$ Hz, $^3J_{\text{PH}} = 15.5$ Hz, ArCH₂N), 4.02 (dd, 2H, $^2J_{\text{HH}} = 11.5$ Hz, $^3J_{\text{PH}} = 15.3$ Hz, ArCH₂N), 3.42, 3.31 (m, 4H, NCH₂). ^{13}C NMR (500 MHz, CDCl₃, ppm): δ 150.61 (d, $^2J_{\text{PC}} = 5.0$ Hz, C₆), 128.96 (s, C₄), 126.90 (s, C₂), 123.63 (s, C₃), 121.85 (t, $^3J_{\text{PC}} = 10.4$ Hz, C₁), 119.11 (t, $^3J_{\text{PC}} = 9.5$ Hz, C₅), 53.27 (s, ArCH₂N), 52.52 (s, NCH₂).

Compound **3a** was crystallized from acetonitrile. Yield: 1.12 g (69%). Mp: 302 °C. Anal. Calcd for C₁₆H₁₆O₂N₆P₄Cl₄: C, 32.57; H, 2.73; N, 14.24. Found: C, 32.61; H, 2.80; N, 14.16. APIES-MS (fragments are based on ³⁵Cl, Ir %): *m/z* 589 ([MH]⁺, 68). FTIR (KBr, cm⁻¹): ν 3077 (asymm), 3019 (symm, C–H arom), 2932, 2863 (C–H aliph), 1582 (C=C), 1283 (asymm), 1167 (symm, P=N), 539 (asymm), 492 (symm, PCl). ^1H NMR (500 MHz, CDCl₃, ppm): δ 7.40 (m, 2H, H₄), 7.35 (d, 2H, H₅), 7.29 (m, 2H, H₃), 7.26 (d, 2H, H₂), 4.69 (dd, 2H, $^2J_{\text{HH}} = 10.3$ Hz, $^3J_{\text{PH}} = 14.9$ Hz, ArCH₂N), 3.68 (dd, 2H, $^2J_{\text{HH}} = 10.4$ Hz, $^3J_{\text{PH}} = 15.4$ Hz, ArCH₂N), 3.31, 3.04 (m, 4H, NCH₂). ^{13}C NMR (500 MHz, CDCl₃, ppm): δ 148.42 (d, $^2J_{\text{PC}} = 4.7$ Hz, C₆), 132.58 (s, C₂), 130.19 (s, C₄), 127.52 (t, $^3J_{\text{PC}} = 7.3$ Hz, C₁), 126.13 (s, C₃), 123.50 (t, $^3J_{\text{PC}} = 6.7$ Hz, C₅), 44.32 (d, $^2J_{\text{PC}} = 12.0$ Hz, NCH₂), 43.72 (s, ArCH₂N).

sas 2b and asa 3b. The workup procedure was similar to that of compounds **2a** and **3a**, using **1b** (1.50 g, 5.00 mmol), K₂CO₃ (2.90 g, 21.00 mmol), N₄P₄Cl₈ (2.43 g, 5.00 mmol), and triethylamine (5.90 mL). The products, **2b** and **3b**, were purified by column chromatography with toluene.

Data for **2b**. Yield: 0.44 g (29%). Mp: 218 °C. Anal. Calcd for C₁₇H₁₈N₆O₂P₄Cl₄: C, 33.80; H, 3.00; N, 13.91. Found: C, 33.91; H, 3.12; N, 13.94. APIES-MS (fragments are based on ³⁵Cl, Ir %): *m/z* 603 ([MH]⁺, 71). FTIR (KBr, cm⁻¹): ν 3082 (asymm), 3021 (symm, C–H arom), 2947, 2850 (C–H aliph), 1588 (C=C), 1276 (asymm), 1186 (symm, P=N), 546 (asymm), 484 (symm, PCl). ^1H NMR (500 MHz, CDCl₃, ppm): δ 7.25 (m, 2H, H₄), 7.05 (m, 6H, H₂, H₃, H₅), 4.46 (dd, 2H, $^2J_{\text{HH}} = 9.0$ Hz, $^3J_{\text{PH}} = 15.3$ Hz, ArCH₂N), 4.14 (dd, 2H, $^2J_{\text{HH}} = 8.9$ Hz, $^3J_{\text{PH}} = 15.2$ Hz, ArCH₂N), 3.41 (m, 4H, NCH₂), 1.81, 1.71 (m, 2H, NCH₂CH₂). ^{13}C NMR (500 MHz, CDCl₃, ppm): δ 151.05 (t, $^3J_{\text{PC}} = 5.1$ Hz, C₆), 129.17 (s, C₄), 126.81 (s, C₂), 123.61 (s, C₃), 123.27 (t, $^3J_{\text{PC}} = 9.4$ Hz, C₁), 119.23 (t, $^3J_{\text{PC}} = 8.7$ Hz, C₅), 50.54 (s, ArCH₂N), 45.90 (s, NCH₂), 27.11 (s, NCH₂CH₂).

Data for **3b**. Yield: 0.95 g (63%). Mp: 267 °C. Anal. Calcd for C₁₇H₁₈N₆O₂P₄Cl₄: C, 33.80; H, 3.00; N, 13.91. Found: C, 33.77; H, 2.91; N, 13.97. APIES-MS (fragments are based on ³⁵Cl, Ir %): *m/z* 603 ([MH]⁺, 85). FTIR (KBr, cm⁻¹): ν 3092 (asymm), 3025 (symm, C–H arom), 2955, 2856 (C–H aliph), 1584 (C=C), 1291 (asymm), 1170 (symm, P=N), 576 (asymm), 480 (symm, PCl). ^1H NMR (500 MHz, CDCl₃, ppm): δ 7.49 (m, 2H, H₄), 7.32 (m, 2H, H₅), 7.30 (d, 2H, H₂), 7.28 (d, 2H, H₃), 4.62 (dd, 2H, $^2J_{\text{HH}} = 11.5$ Hz, $^3J_{\text{PH}} = 15.3$ Hz, ArCH₂N), 3.71 (dd, 2H, $^2J_{\text{HH}} = 13.4$ Hz, $^3J_{\text{PH}} = 15.4$ Hz, ArCH₂N), 3.12 (m, 4H, NCH₂), 1.75 (m, 2H, NCH₂CH₂). ^{13}C NMR (500 MHz, CDCl₃, ppm): δ 148.09 (d, $^2J_{\text{PC}} = 4.8$ Hz, C₆), 132.12 (s, C₂), 130.31 (t, $^3J_{\text{PC}} = 7.0$ Hz, C₁), 130.01 (s, C₄), 126.52 (s, C₃), 122.58 (t, $^3J_{\text{PC}} = 6.9$ Hz, C₅), 48.60 (s, NCH₂), 46.21 (d, $^2J_{\text{PC}} = 3.3$ Hz, ArCH₂N), 26.13 (d, $^3J_{\text{PC}} = 7.2$ Hz, NCH₂CH₂).

sas 2g and bicyclo-2,6-as 4g. The workup procedure was similar to that of compounds **2a** and **3a**, using **1g** (1.50 g, 5.00 mmol), K₂CO₃ (2.46 g, 25.00 mmol), N₄P₄Cl₈ (2.32 g, 5.00 mmol), and triethylamine (5.60 mL). The products, **2g** and **4g**, were purified by column chromatography with toluene.

Data for **2g**. Yield: 0.10 g (6%). Mp: 158 °C. Anal. Calcd for C₁₈H₂₀N₆O₂P₄Cl₄: C, 34.98; H, 3.26; N, 13.59. Found: C, 35.28; H, 3.26; N, 13.26. APIES-MS (fragments are based on ³⁵Cl, Ir %): *m/z*

617 ([MH]⁺, 79). FTIR (KBr, cm⁻¹): ν 3080 (asymm), 3022 (symm, C–H arom), 2952, 2853 (C–H aliph), 1587 (C=C), 1272 (asymm), 1185 (symm, P=N), 566 (asymm), 484 (symm, PCl). ¹H NMR (500 MHz, CDCl₃, ppm): δ 7.20 (m, 2H, H₄), 7.06 (m, 6H, H₂, H₃, H₅), 4.46 (d, 4H, ³J_{PH} = 14.4 Hz, ArCH₂N), 3.13 (m, 4H, NCH₂), 1.62 (m, 4H, NCH₂CH₂). ¹³C NMR (500 MHz, CDCl₃): δ 150.08 (t, ²J_{PC} = 5.4 Hz, C₆), 131.06 (s, C₄), 129.98 (s, C₂), 125.53 (s, C₃), 123.60 (t, ³J_{PC} = 9.5 Hz, C₁), 123.91 (t, ³J_{PC} = 8.8 Hz, C₅), 51.13 (s, ArCH₂N), 47.94 (s, NCH₂), 26.86 (s, NCH₂CH₂).

Data for **4g**. Yield: 0.26 g (17%). Mp: 262 °C. Anal. Calcd for C₁₈H₂₁N₆O₂P₄Cl₅: C, 33.03; H, 3.23; N, 12.84. Found: C, 33.13; H, 3.24; N, 12.93. APIES-MS (fragments are based on ³⁵Cl, Ir %): *m/z* 653 ([MH]⁺, 35). FTIR (KBr, cm⁻¹): ν 3327 (O–H), 3079 (asymm), 3026 (symm, C–H arom), 2947, 2848 (C–H aliph), 1585 (C=C), 1262 (asymm), 1173 (symm, P=N), 568 (asymm), 489 (symm, PCl). ¹H NMR (500 MHz, CDCl₃, ppm): δ 7.91 (b, H, ArOH), 7.36 (m, H, H₅), 7.30 (dd, H, H₂), 7.18 (d, H, H'₅), 7.15 (dd, H, H₄), 7.09 (d, H, H'₂), 7.03 (dd, H, H'₄), 6.83 (dd, H, H₃), 6.75 (dd, H, H'₃), 4.32 (d, 2H, ³J_{PH} = 12.5 Hz, ArCH₂N), 4.24 (d, 2H, ³J_{PH} = 8.6 Hz, ArCH₂N), 3.12 (m, 4H, NCH₂), 1.59, 1.27 (m, 4H, NCH₂CH₂). ¹³C NMR (500 MHz, CDCl₃): δ 155.81 (s, C'₆), 150.22 (d, ²J_{PC} = 12.1 Hz, C₆), 132.72 (s, C₄), 130.12 (s, C₄), 129.91 (d, ⁴J_{PC} = 2.2 Hz, C'₂), 125.62 (d, ⁴J_{PC} = 2.1 Hz, C₂), 129.35 (d, ³J_{PC} = 6.9 Hz, C'₁), 123.10 (d, ³J_{PC} = 6.1 Hz, C₁), 129.94 (s, C'₃), 120.42 (t, ³J_{PC} = 3.6 Hz, C₅), 119.55 (s, C'₃), 116.09 (s, C₃), 48.31 (d, ²J_{PC} = 4.7 Hz, ArC'H₂N), 45.82 (d, ²J_{PC} = 6.7 Hz, NC'H₂), 44.36 (d, ²J_{PC} = 6.0 Hz, ArCH₂N), 42.72 (d, ²J_{PC} = 7.9 Hz, NCH₂), 27.63 (s, NCH₂CH₂), 24.01 (s, NCH₂CH₂).

sas 2h. The workup procedure was similar to that of compounds **2a** and **3a**, using **1h** (1.50 g, 4.50 mmol), K₂CO₃ (2.53 g, 19.00 mmol), N₄P₄Cl₈ (2.10 g, 4.50 mmol), and triethylamine (3.70 mL). The product **2h** was purified by column chromatography with toluene. Yield: 0.12 g (4%). Mp: 203 °C. Anal. Calcd for C₂₀H₂₄N₆O₂P₄Cl₄: C, 37.18; H, 3.74; N, 13.01. Found: C, 37.47; H, 3.75; N, 13.08. APIES-MS (fragments are based on ³⁵Cl, Ir %): *m/z* 645 ([MH]⁺, 37). FTIR (KBr, cm⁻¹): ν 3078 (asymm), 3042 (symm, C–H arom), 2957, 2846 (C–H aliph), 1584 (C=C), 1280 (asymm), 1183 (symm, P=N), 570 (asymm), 489 (symm, PCl). ¹H NMR (500 MHz, CDCl₃, ppm): δ 7.24 (m, 2H, H₄), 7.05 (m, 6H, H₂, H₃, H₅), 4.34 (d, 4H, ³J_{PH} = 14.8 Hz, ArCH₂N), 3.18 (m, 4H, NCH₂), 1.61 (m, 8H, NCH₂CH₂ and NCH₂CH₂CH₂). ¹³C NMR (500 MHz, CDCl₃, ppm): δ 151.64 (t, ²J_{PC} = 6.9 Hz, C₆), 128.79 (s, C₄), 127.27 (s, C₂), 123.20 (s, C₃), 122.52 (t, ³J_{PC} = 11.2 Hz, C₁), 119.15 (t, ³J_{PC} = 9.3 Hz, C₅), 46.80 (s, ArCH₂N), 46.43 (s, NCH₂), 27.43 (d, ³J_{PC} = 6.1 Hz, NCH₂CH₂), 23.44 (s, NCH₂CH₂CH₂).

sas 2c. A solution of pyrrolidine (0.60 mL, 6.80 mmol) in dry THF (50 mL) was slowly added to a stirred solution of triethylamine (0.40 mL) and **2a** (0.40 g, 0.70 mmol) in dry THF (100 mL) at room temperature. The solution was heated to reflux for 12 h under an argon atmosphere. The precipitated triethylamine hydrochloride was filtered off, and the solvent was evaporated. The product was purified by column chromatography with toluene–THF (1:1), and a white powder was crystallized from acetonitrile–THF (3:1). Yield: 0.36 g (73%). Mp: 203 °C. Anal. Calcd for C₃₂H₄₈O₂N₁₀P₄ · H₂O: C, 51.43; H, 6.70; N, 18.75. Found: C, 51.81; H, 6.39; N, 18.11. APIES-MS (fragments are based on ³⁵Cl, Ir %): *m/z* 729 ([MH]⁺, 100). FTIR (KBr, cm⁻¹): ν 3415 (O–H), 3064 (asymm), 3039 (symm, C–H arom), 2958, 2864 (C–H aliph), 1581 (C=C), 1295 (asymm), 1180 (symm, P=N), 571 (asymm), 503 (symm, PCl). ¹H NMR (500 MHz, toluene, ppm): δ 6.93 (m, 4H, H₄, H₅), 6.77 (m, 4H, H₂, H₃), 3.54 (dd, 2H, ²J_{HH} = 10.7 Hz, ³J_{PH} = 14.7 Hz, ArCH₂N), 4.56 (d, 2H, ³J_{PH} = 14.8 Hz, ArCH₂N), 3.08, 2.80 [m, 4H, NCH₂ (ansa)], 3.22 [m, 16H, NCH₂ (pyrr)], 1.65 [m, 16H, NCH₂CH₂ (pyrr)]. ¹³C NMR (500 MHz, CDCl₃, ppm): δ 151.59 (d, ²J_{PC} = 4.8 Hz, C₆), 127.86 (s, C₄), 126.58 (s, C₂), 122.96 (t, ³J_{PC} = 8.2 Hz, C₁), 121.86 (s, C₃), 118.78 (t, ³J_{PC} = 9.2 Hz, C₅), 53.43 (s, ArCH₂N), 52.27 [s, NCH₂ (ansa)], 46.76, 46.65 [s, NCH₂ (pyrr)], 26.59 [s, ³J_{PC} = 9.7 Hz, NCH₂CH₂ (pyrr)].

sas 2d. The workup procedure was similar to that of compound **2c**, using **2b** (0.50 g, 0.80 mmol), pyrrolidine (0.70 mL, 8.30 mmol), and triethylamine (0.45 mL). The oily residue was purified by column

chromatography with benzene–THF (1:1) and crystallized from acetonitrile–THF (3:1). Yield: 0.43 g (70%). Mp: 180 °C. Anal. Calcd for C₃₃H₅₀O₂N₁₀P₄: C, 53.37; H, 6.79; N, 18.86. Found: C, 53.49; H, 6.70; N, 18.79. APIES-MS (fragments are based on ³⁵Cl, Ir %): *m/z* 743 ([MH]⁺, 100). FTIR (KBr, cm⁻¹): ν 3077 (asymm), 3043 (symm, C–H arom), 2958, 2848 (C–H aliph), 1587 (C=C), 1281 (asymm), 1166 (symm, P=N), 566 (asymm), 489 (symm, PCl). ¹H NMR (500 MHz, CDCl₃, ppm): δ 7.13 (m, 2H, H₄), 7.01 (m, 2H, H₂), 6.92 (m, 4H, H₃, H₅), 4.32 (dd, 2H, ²J_{HH} = 10.2 Hz, ³J_{PH} = 15.6 Hz, ArCH₂N), 4.18 (dd, 2H, ²J_{HH} = 8.2 Hz, ³J_{PH} = 15.9 Hz, ArCH₂N), 3.50, 3.31 [m, 4H, NCH₂ (ansa)], 3.11 [m, 16H, NCH₂ (pyrr)], 1.79 [m, 2H, NCH₂CH₂ (ansa)], 1.62 [m, 16H, NCH₂CH₂ (pyrr)]. ¹³C NMR (500 MHz, CDCl₃, ppm): δ 151.80 (d, ²J_{PC} = 4.9 Hz, C₆), 127.81 (s, C₄), 126.55 (s, C₂), 122.93 (t, ³J_{PC} = 7.9 Hz, C₁), 121.79 (s, C₃), 118.83 (t, ³J_{PC} = 7.2 Hz, C₅), 50.51 (s, ArCH₂N), 46.37 [s, NCH₂ (ansa)], 46.29, 46.47 [s, NCH₂ (pyrr)], 27.61 [s, NCH₂CH₂ (ansa)], 26.46 [t, ³J_{PC} = 9.5 Hz, NCH₂CH₂ (pyrr)].

sas 2e. A solution of morpholine (0.60 mL, 6.80 mmol) in dry THF (50 mL) was slowly added to a stirred solution of triethylamine (0.40 mL) and **2a** (0.40 g, 0.70 mmol) in dry THF (100 mL) at room temperature. The solution was heated to reflux for 10 h with argon being passed over the mixture. The precipitated amine hydrochloride was filtered off, and the solvent was evaporated at reduced pressure. The oily residue was purified by column chromatography with toluene–THF (1:1) and crystallized from acetonitrile–THF (3:1). Yield: 0.36 g (67%). Mp: 197 °C. Anal. Calcd for C₃₂H₄₈O₆N₁₀P₄C₇H₈ (toluene): C, 52.94; H, 6.33; N, 15.84. Found: C, 52.19; H, 6.29; N, 16.39. APIES-MS (fragments are based on ³⁵Cl, Ir %): *m/z* 793 ([MH]⁺, 100). FTIR (KBr, cm⁻¹): ν 3063 (asymm), 3029 (symm, C–H arom), 2957, 2849 (C–H aliph), 1585 (C=C), 1294 (asymm), 1180 (symm, P=N), 538 (asymm), 486 (symm, PCl). ¹H NMR (500 MHz, CDCl₃, ppm): δ 7.20 (m, 2H, H₄), 7.03 (m, 2H, H₂), 6.96 (m, 2H, H₃), 6.94 (m, 2H, H₅), 4.51 (dd, 2H, ²J_{HH} = 10.6 Hz, ³J_{PH} = 15.3 Hz, ArCH₂N), 4.01 (dd, 2H, ²J_{HH} = 10.6 Hz, ³J_{PH} = 15.2 Hz, ArCH₂N), 3.62 [m, 16H, NCH₂CH₂ (mor)], 3.32, 3.11 [m, 4H, NCH₂ (ansa)], 3.11 [m, 16H, NCH₂ (mor)]. ¹³C NMR (500 MHz, CDCl₃, ppm): δ 150.21 (d, ²J_{PC} = 4.8 Hz, C₆), 128.32 (s, C₄), 126.83 (s, C₂), 122.45 (s, C₃), 118.82 (t, ³J_{PC} = 6.7 Hz, C₅), 112.94 (t, ³J_{PC} = 7.3 Hz, C₁), 67.31 [t, ³J_{PC} = 9.6 Hz, NCH₂CH₂ (mor)], 53.24 (s, ArCH₂N), 52.22 [s, NCH₂ (ansa)], 45.16, 44.92 [s, NCH₂ (mor)].

sas 2f. The workup procedure was similar to that of compound **2e**, using **2b** (0.50 g, 0.80 mmol), morpholine (0.70 mL, 8.30 mmol), and triethylamine (0.45 mL). Yield: 0.41 g (62%). Mp: 147 °C. Anal. Calcd for C₃₃H₅₀O₆N₁₀P₄: C, 49.14; H, 6.25; N, 17.37. Found: C, 50.01; H, 6.48; N, 17.96. APIES-MS (fragments are based on ³⁵Cl, Ir %): *m/z* 808 ([M + 2H]⁺, 100). FTIR (KBr, cm⁻¹): ν 3066 (asymm), 3043 (symm, C–H arom), 2956, 2848 (C–H aliph), 1589 (C=C), 1288 (asymm), 1184 (symm, P=N), 538 (asymm), 489 (symm, PCl). ¹H NMR (500 MHz, CDCl₃, ppm): δ 7.26 (m, 2H, H₄), 7.06 (m, 2H, H₂), 6.98 (m, 2H, H₃), 6.95 (m, 2H, H₅), 4.43 (dd, 2H, ²J_{HH} = 9.4 Hz, ³J_{PH} = 15.2 Hz, ArCH₂N), 4.25 (dd, 2H, ²J_{HH} = 9.3 Hz, ³J_{PH} = 15.1 Hz, ArCH₂N), 3.72 [t, 16H, NCH₂CH₂ (mor)], 3.40, 3.25 [m, 4H, NCH₂ (ansa)], 3.12 [m, 16H, NCH₂ (mor)], 1.82, 1.63 [m, 2H, NCH₂CH₂ (ansa)]. ¹³C NMR (500 MHz, CDCl₃, ppm): δ 151.43 (d, ²J_{PC} = 4.7 Hz, C₆), 128.25 (s, C₄), 126.69 (s, C₂), 123.56 (t, ³J_{PC} = 8.4 Hz, C₁), 122.34 (s, C₃), 119.03 (d, ³J_{PC} = 8.6 Hz, C₅), 67.42 [t, ³J_{PC} = 9.8 Hz, NCH₂CH₂ (mor)], 50.39 (s, ArCH₂N), 45.91 [s, NCH₂ (ansa)], 45.23, 45.12 [s, NCH₂ (mor)], 30.37 [s, NCH₂CH₂ (ansa)].

asa 3a. The workup procedure was similar to that of compound **2c**, using **3c** (0.80 g, 1.35 mmol), pyrrolidine (1.10 mL, 13.50 mmol), and triethylamine (0.80 mL). The oily residue was purified by column chromatography with benzene–THF (1:1) and crystallized from acetonitrile–THF (3:1). Yield: 0.76 g (85%). Mp: 308 °C. Anal. Calcd for C₂₄H₃₂O₂N₈P₄Cl₂: C, 43.72; H, 4.89; N, 16.99. Found: C, 44.39; H, 5.00; N, 16.48. APIES-MS (fragments are based on ³⁵Cl, Ir %): *m/z* 659 ([MH]⁺, 100). FTIR (KBr, cm⁻¹): ν 3072 (asymm), 3029 (symm, C–H arom), 2955, 2857 (C–H aliph), 1582 (C=C), 1272 (asymm), 1177 (symm, P=N), 549 (PCl). ¹H NMR (500 MHz, CDCl₃, ppm): δ 7.36 (m, 4H, H₄ and H₅), 7.19 (m, 4H, H₂ and H₃), 4.68 (dd, 2H, ²J_{HH} = 14.8 Hz, ³J_{PH} = 15.1 Hz, ArCH₂N), 3.63 (dd, 2H, ²J_{HH} = 14.8

Table 1. Crystallographic Details

	2b	3a	3b	3e	4g
empirical formula	C ₁₇ H ₁₈ Cl ₄ N ₆ O ₂ P ₄	C ₁₆ H ₁₆ Cl ₄ N ₆ O ₂ P ₄	C ₁₇ H ₁₈ Cl ₄ N ₆ O ₂ P ₄	C ₂₄ H ₃₂ Cl ₂ N ₈ O ₄ P ₄	C ₁₈ H ₂₁ Cl ₅ N ₆ O ₂ P ₄
fw	604.05	590.03	604.05	691.36	654.54
cryst syst	orthorhombic	monoclinic	orthorhombic	monoclinic	monoclinic
space group	<i>Pbmm</i>	<i>C2/c</i>	<i>P2₁2₁2₁</i>	<i>P2₁/c</i>	<i>C2/c</i>
<i>a</i> (Å)	9.4186(3)	23.3455(4)	9.9387(3)	14.6946(2)	18.241(3)
<i>b</i> (Å)	12.1307(4)	8.4787(2)	11.7933(3)	8.7960(1)	8.516(2)
<i>c</i> (Å)	21.1905(7)	24.5024(5)	20.7778(6)	23.8967(3)	35.359(5)
α (deg)	90.00	90.00	90.00	90.00	90.00
β (deg)	90.00	106.38(5)	90.00	98.723(1)	102.90(2)
γ (deg)	90.00	90.00	90.00	90.00	90.00
<i>V</i> (Å ³)	2421.10(14)	4653.1(12)	2435.37(12)	3053.01(7)	5354.0(18)
<i>Z</i>	4	8	4	4	8
μ (Mo <i>K</i> α) (cm ⁻¹)	7.83	8.13	7.79	4.69	8.12
ρ (calcd) (g/cm ³)	1.657	1.684	1.647	1.504	1.624
no. of total reflns	3079	5803	5984	7594	6616
no. of unique reflns	2443	5133	5850	5683	5085
<i>R</i> _{int}	0.0353	0.0259	0.0191	0.0743	0.1097
2θ _{max} (deg)	56.74	56.68	56.66	56.66	57.58
<i>T</i> _{min} / <i>T</i> _{max}	0.7990/0.8591	0.7264/0.8164	0.7407/0.8000	0.8346/0.9416	0.7643/0.8416
no. of param	154	289	298	379	320
<i>R</i> ₁ [<i>F</i> ² > 2 σ (<i>F</i> ²)]	0.0277	0.0244	0.0210	0.0350	0.0483
w <i>R</i> ₂	0.0706	0.0684	0.0555	0.0805	0.0914

Hz, ³J_{PH} = 15.3 Hz, ArCH₂N), 3.78, 2.96 [m, 4H, NCH₂ (spiro)], 3.41, 3.26 [m, 8H, NCH₂ (pyrr)], 1.91 [m, 8H, NCH₂CH₂ (pyrr)]. ¹³C NMR (500 MHz, CDCl₃, ppm): δ 149.66 (d, ²J_{PC} = 5.7 Hz, C₆), 132.27 (s, C₂), 129.64 (s, C₄), 127.97 (t, ³J_{PC} = 7.2 Hz, C₁), 125.12 (s, C₃), 123.56 (t, ³J_{PC} = 6.6 Hz, C₅), 46.40 [d, ²J_{PC} = 5.0 Hz, NCH₂ (pyrr)], 44.33 [d, ²J_{PC} = 11.6 Hz, NCH₂ (spiro)], 43.51 (s, ArCH₂N), 26.52 [d, ³J_{PC} = 9.7 Hz, NCH₂CH₂ (pyrr)].

Microwave-Assisted Synthesis of 3c. Pyrrolidine (1.10 mL, 13.50 mmol) in dry THF (50 mL) was slowly added to a stirred solution of triethylamine (0.80 mL) and **3a** (0.80 g, 1.35 mmol) in dry THF (100 mL). The mixture was refluxed for 0.50 h, and triethylamine hydrochloride was filtered off. THF was evaporated, and the crude product was purified by column chromatography with benzene–THF (1:1) and crystallized from acetonitrile–THF (3:1). Yield: 0.85 g (95%).

Compound **3c** was also synthesized in toluene and *o*-xylene. The workup procedure was similar to that of the THF solvent, whereas the mixture was refluxed for 0.75 h in toluene [yield: 0.80 g (90%)] and in *o*-xylene for 1 h [yield: 0.70 g (78%)].

asa 3d. The workup procedure was similar to that of compound **2c**, using **3b** (0.80 g, 1.30 mmol), pyrrolidine (1.10 mL, 13.00 mmol), and triethylamine (0.75 mL). The oily residue was purified by column chromatography with THF and crystallized from acetonitrile–THF (3:1). Yield: 0.74 g (83%). Mp: 302 °C. Anal. Calcd for C₂₅H₃₄O₂N₈P₄Cl₂: C, 44.59; H, 5.09; N, 16.64. Found: C, 45.26; H, 5.13; N, 16.40. APIES-MS (fragments are based on ³⁵Cl, Ir %): *m/z* 673 ([MH]⁺, 100). FTIR (KBr, cm⁻¹): ν 3057 (asymm), 3030 (symm, C–H arom), 2922, 2852 (C–H aliph), 1581 (C=C), 1268 (asymm), 1176 (symm, P=N), 544 (P=Cl). ¹H NMR (500 MHz, CDCl₃, ppm): δ 7.35 (dd, 2H, H₄), 7.28 (d, 4H, H₂, H₃), 7.18 (dd, 2H, H₃), 4.81 (dd, 2H, ²J_{HH} = 8.9 Hz, ³J_{PH} = 15.5 Hz, ArCH₂N), 3.56 (dd, 2H, ²J_{HH} = 10.7 Hz, ³J_{PH} = 15.7 Hz, ArCH₂N), 3.33, 3.27 [m, 8H, NCH₂ (pyrr)], 3.19, 3.10 [m, 4H, NCH₂ (spiro)], 1.90 [m, 8H, NCH₂CH₂ (pyrr)], 1.77 [m, 2H, NCH₂CH₂ (spiro)]. ¹³C NMR (500 MHz, CDCl₃, ppm): δ 149.26 (d, ²J_{PC} = 8.4 Hz, C₆), 131.09 (s, C₂), 130.45 (t, ³J_{PC} = 8.2 Hz, C₁), 129.42 (s, C₄), 125.23 (s, C₃), 122.91 (t, ³J_{PC} = 6.8 Hz, C₅), 48.92 [s, NCH₂ (spiro)], 47.28 (d, ²J_{PC} = 3.9 Hz, ArCH₂N), 46.52 [d, ²J_{PC} = 5.0 Hz, NCH₂ (pyrr)], 26.48 [d, ³J_{PC} = 9.4 Hz, NCH₂CH₂ (pyrr)], 26.35 [d, ³J_{PC} = 7.4 Hz, NCH₂CH₂ (spiro)].

asa 3e. The workup procedure was similar to that of compound **2e**, using **3a** (0.80 g, 1.35 mmol), morpholine (1.20 mL, 13.60 mmol),

and triethylamine (0.75 mL). The oily residue was purified by column chromatography with benzene–THF (1:1) and crystallized from acetonitrile. Yield: 0.70 g (74%). Mp: >320 °C. Anal. Calcd for C₂₄H₃₂O₄N₈P₄Cl₂: C, 41.70; H, 4.67; N, 16.21. Found: C, 41.92; H, 4.61; N, 16.12. APIES-MS (fragments are based on ³⁵Cl, Ir %): *m/z* 691 ([MH]⁺, 100). FTIR (KBr, cm⁻¹): ν 3073 (asymm), 3029 (symm, C–H arom), 2959, 2846 (C–H aliph), 1583 (C=C), 1286 (asymm), 1179 (symm, P=N), 538 (P=Cl). ¹H NMR (500 MHz, CDCl₃, ppm): δ 7.37 (m, 4H, H₄ and H₅), 7.21 (m, 4H, H₂ and H₃), 4.64 (dd, 2H, ²J_{HH} = 8.9 Hz, ³J_{PH} = 15.3 Hz, ArCH₂N), 3.78, 3.72 [m, 8H, NCH₂CH₂ (mor)], 3.63 (dd, 2H, ²J_{HH} = 13.7 Hz, ³J_{PH} = 15.3 Hz, ArCH₂N), 3.41, 3.28 [m, 8H, NCH₂ (mor)], 3.24, 2.97 [m, 4H, NCH₂ (spiro)]. ¹³C NMR (500 MHz, CDCl₃, ppm): δ 149.40 (d, ²J_{PC} = 4.9 Hz, C₆), 132.18 (s, C₂), 129.93 (s, C₄), 128.03 (t, ³J_{PC} = 7.4 Hz, C₁), 125.22 (s, C₃), 123.22 (t, ³J_{PC} = 6.9 Hz, C₅), 67.12 [t, ³J_{PC} = 9.2 Hz, NCH₂CH₂ (mor)], 44.77 (s, NCH₂ (mor)], 44.37 [d, ²J_{PC} = 12.0 Hz, NCH₂ (spiro)], 43.41 (s, ArCH₂N).

asa 3f. The workup procedure was similar to that of compound **2e**, using **3b** (0.70 g, 1.15 mmol), morpholine (1.00 mL, 11.50 mmol), and triethylamine (0.65 mL). The oily residue was purified by column chromatography with THF and crystallized from chloroform. Yield: 0.61 g (75%). Mp: 270 °C. Anal. Calcd for C₂₅H₃₄O₄N₈P₄Cl₂: C, 42.57; H, 4.86; N, 15.89. Found: C, 42.96; H, 4.88; N, 15.70. APIES-MS (fragments are based on ³⁵Cl, Ir %): *m/z* 705 ([MH]⁺, 100). FTIR (KBr, cm⁻¹): ν 3062 (asymm), 3037 (symm, C–H arom), 2954, 2846 (C–H aliph), 1583 (C=C), 1288 (asymm), 1176 (symm, P=N), 551 (P=Cl). ¹H NMR (500 MHz, CDCl₃, ppm): δ 7.39 (t, 2H, H₄), 7.32 (t, 4H, H₂ and H₃), 7.21 (t, 2H, H₃), 4.76 (dd, 2H, ²J_{HH} = 10.7 Hz, ³J_{PH} = 15.1 Hz, ArCH₂N), 3.78, 3.71 [m, 8H, NCH₂CH₂ (mor)], 3.57 (dd, 2H, ²J_{HH} = 11.1 Hz, ³J_{PH} = 15.0 Hz, ArCH₂N), 3.36, 3.27 [m, 8H, NCH₂ (mor)], 3.18, 3.08 [m, 4H, NCH₂ (spiro)], 1.77 [m, 2H, NCH₂CH₂ (spiro)]. ¹³C NMR (500 MHz, CDCl₃, ppm): δ 149.16 (d, ²J_{PC} = 8.4 Hz, C₆), 131.34 (s, C₂), 130.31 (d, ³J_{PC} = 8.4 Hz, C₁), 129.12 (s, C₄), 125.25 (s, C₃), 122.81 (d, ³J_{PC} = 7.5 Hz, C₅), 66.92 [d, ³J_{PC} = 9.6 Hz, NCH₂CH₂ (mor)], 48.81 [d, ²J_{PC} = 4.7 Hz, NCH₂ (spiro)], 47.32 (s, ArCH₂N), 44.83 [s, NCH₂ (mor)], 26.45 [d, ³J_{PC} = 9.4 Hz, NCH₂CH₂ (spiro)].

X-ray Crystal Structure Determinations. The colorless crystals of compounds **2b**, **3a**, **3b**, **3e**, and **4g** were crystallized from acetonitrile at room temperature. The crystallographic data are given in Table 1, and selected bond lengths and angles are listed in Table 2.

Table 2. Selected Bond Lengths (Å) and Angles (deg) for 2b, 3a, 3b, 3e, and 4g

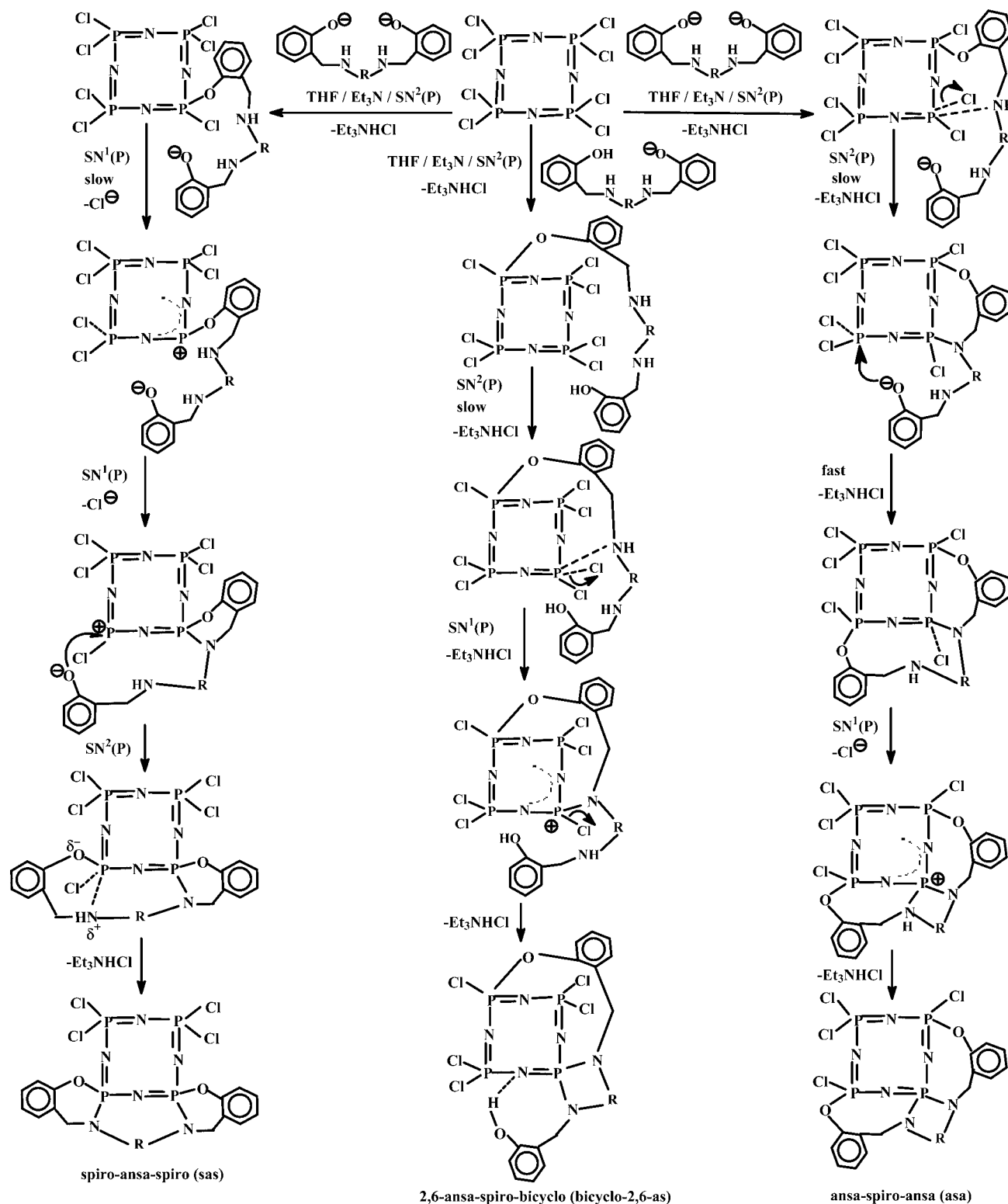
	2b		3a	3b	3e	4g
P1–N1	1.576(1)	P1–N1	1.554(1)	1.546(1)	1.565(1)	1.577(2)
P1–N4	1.594(1)	P1–N4	1.579(1)	1.581(1)	1.549(1)	1.573(2)
		P2–N1	1.603(1)	1.610(1)	1.598(1)	1.544(2)
		P2–N2	1.603(1)	1.598(1)	1.605(1)	1.544(2)
		P3–N3	1.576(1)	1.575(1)	1.555(1)	1.608(2)
		P3–N2	1.561(1)	1.550(1)	1.561(1)	1.640(2)
P4–N3	1.563(1)	P4–N3	1.564(1)	1.566(1)	1.593(1)	1.562(2)
P4–N4	1.560(1)	P4–N4	1.567(1)	1.561(1)	1.584(1)	1.551(2)
P1–N5	1.626(1)	P1–N5				
P2–N5		P2–N5	1.645(1)	1.650(1)	1.639(1)	
		P2–N6	1.645(1)	1.633(1)	1.649(1)	
P3–N5		P3–N5				1.637(2)
P3–N6		P3–N6				1.612(2)
P4–Cl1	1.999(6)	P1–Cl1	2.009(5)	2.024(5)	2.029(7)	1.963(7)
P4–Cl2	2.024(6)	P3–Cl2	2.011(5)	2.032(6)	2.033(7)	
		P4–Cl3	2.009(5)	2.009(6)		
		P4–Cl4	1.999(5)	2.005(6)		2.022(8)
		P4–Cl5				2.025(9)
		P2–Cl2				2.033(8)
		P2–Cl3				2.016(9)
N1–P1–N4	114.00(9)	N1–P1–N4	122.21(6)	123.49(7)	125.16(8)	121.29(11)
N5–P2–N6		N5–P2–N6	95.49(7)	104.65(7)	95.05(8)	
N5–P3–N6		N5–P3–N6				103.42(9)
		N1–P2–N2	112.89(6)	112.44(7)	113.09(8)	123.00(11)
N7–P4–N8		N7–P4–N8			102.80(8)	
		N2–P3–N3	123.31(6)	123.71(7)	125.27(8)	113.94(9)
N3–P4–N4	122.57(10)	N3–P4–N4	121.89(7)	122.29(8)	117.64(8)	121.69(10)
N5–P1–N1	118.06(9)	N5–P1–N1				
N5–P2–N1		N5–P2–N1	108.54(6)	110.97(7)	114.93(8)	
N6–P2–N2		N6–P2–N2	115.91(6)	110.73(7)	114.55(8)	
		N6–P2–N1	108.54(6)	110.59(7)	109.12(8)	
N5–P3–N3		N5–P3–N3				106.98(9)
N2–P3–N6		N2–P3–N6				103.10(10)
P3–N3–P4	141.37(14)	P3–N3–P4	129.34(9)	129.52(10)	131.01(11)	129.99(12)
P1–N1–P2	128.77(13)	P1–N1–P2	129.35(7)	132.35(9)	128.81(10)	130.06(13)
		P3–N2–P2	128.27(8)	134.27(9)	128.15(10)	133.64(12)
P1–N4–P4	126.91(10)	P1–N4–P4	128.67(9)	132.65(10)	137.42(10)	127.01(11)

Crystallographic data were recorded on a Bruker Kappa APEXII CCD area-detector diffractometer using Mo K α radiation ($\lambda = 0.71073$ Å) at $T = 100(2)$ K. Absorption corrections by multiscan³⁰ were applied. Structures were solved by direct methods and refined by full-matrix least squares against F^2 using all data.³¹ All non-H atoms were refined anisotropically. In compound **4g**, only the H atom of the OH group was located in a difference Fourier synthesis and refined isotropically [O–H = 0.83(4) Å; $U_{\text{iso}}(\text{H}) = 0.17(2)$ Å²]. The remaining H-atom positions were calculated geometrically at distances of 0.93 Å (CH) and 0.97 Å (CH₂) (for compounds **2b**, **3b**, and **4g**) and 0.95 Å (CH) and 0.99 Å (CH₂) (for compounds **3a** and **3e**) from the parent C atoms; a riding model was used during the refinement process, and the $U_{\text{iso}}(\text{H})$ values were constrained to be $1.2U_{\text{eq}}(\text{carrier atom})$.

RESULTS AND DISCUSSION

Synthesis. All aminopodands [(HOPhCH₂NH)₂R, where R = (CH₂)_{*n*}, with $n = 2$ (**1a**), $n = 3$ (**1b**), $n = 4$ (**1g**), and $n = 6$ (**1h**)] have been prepared by the reduction of bis-(iminopodands) (Schiff bases) with the NaBH₄–borax system.²⁹ The tentative reaction pathways suggested for the reactions of N₄P₄Cl₈ with tetradentate ligands are given in Scheme 2. The possible reaction mechanisms SN²(P) and/or

SN¹(P) are written in the scheme. The reactions of N₄P₄Cl₈ with an equimolar amount of dipotassium salts, (KOPhCH₂NH)₂R, of aminopodands (**1a** and **1b**) afford the novel **sas** (**2a** and **2b**) and **asa** (**3a** and **3b**) tetrachlorocyclotetraphosphazenes in THF, respectively (Scheme 1). On the other hand, the reaction of N₄P₄Cl₈ with an equimolar amount of potassium salts of the long-chain starting compound (**1g**) gives **sas** (**2g**) and the interesting **bicyclo-2,6-as** product (**4g**). Hence, the formation of **4g** indicates that the monopotassium salt of **1g** is present in the reaction mixture of **1g**, K₂CO₃, and N₄P₄Cl₈. However, the equimolar amount of the dipotassium salt of the long-chain starting compound **1h** produces only **sas** (**2h**). The expected **asa** products of N₄P₄Cl₈ with **1g** and **1h** were not obtained in THF. If the alkyl chain lengths increase, the **sas** compounds are the major products, whereas as the alkyl chain lengths decrease, the **asa** derivatives are dominant. The **sas** and **asa** products may occur competitively via SN²(P) or SN¹(P) mechanisms. These compounds are the first examples of cyclotetraphosphazene derivatives with the bulky N₂O₂ donor-type aminopodands, while in the literature,^{5a} there is only one **bicyclo-2,6-as** compound and one **bicyclo-2,6-sas**

Scheme 2. Tentative Reaction Pathways of $N_4P_4Cl_8$ with Aminopodands in THF

compound obtained with spermidine and spermine, respectively. Generally, the yields of *asa* products (**3a** and **3b**) are higher than those of *sas* products (**2a** and **2b**). In addition, the yields of both *sas* (**2a** and **2b**) and *asa* (**3a** and **3b**) phosphazenes also depend on the chain lengths [$R = (CH_2)_n$] of aminopodands. For instance, the yields of both *sas* (**2a**, yield 22%) and *asa* (**3a**, yield 69%) products, which

have the smallest alkyl chains, $R = (CH_2)_2$, are higher than those of *sas* (**2b**, yield 29%) and *asa* (**3b**, yield 63%) products, $R = (CH_2)_3$. Parts a and b of Figure 1 depict the reaction products of $N_3P_3Cl_6$ and $N_4P_4Cl_8$ with the tetradentate ligands (**1a** and **1b**) and **1g**.

If the alkyl chains are $(CH_2)_2$ and $(CH_2)_3$, *sbs* compounds^{7a} are formed with $N_3P_3Cl_6$, but *sbs* compounds with $N_4P_4Cl_8$ are

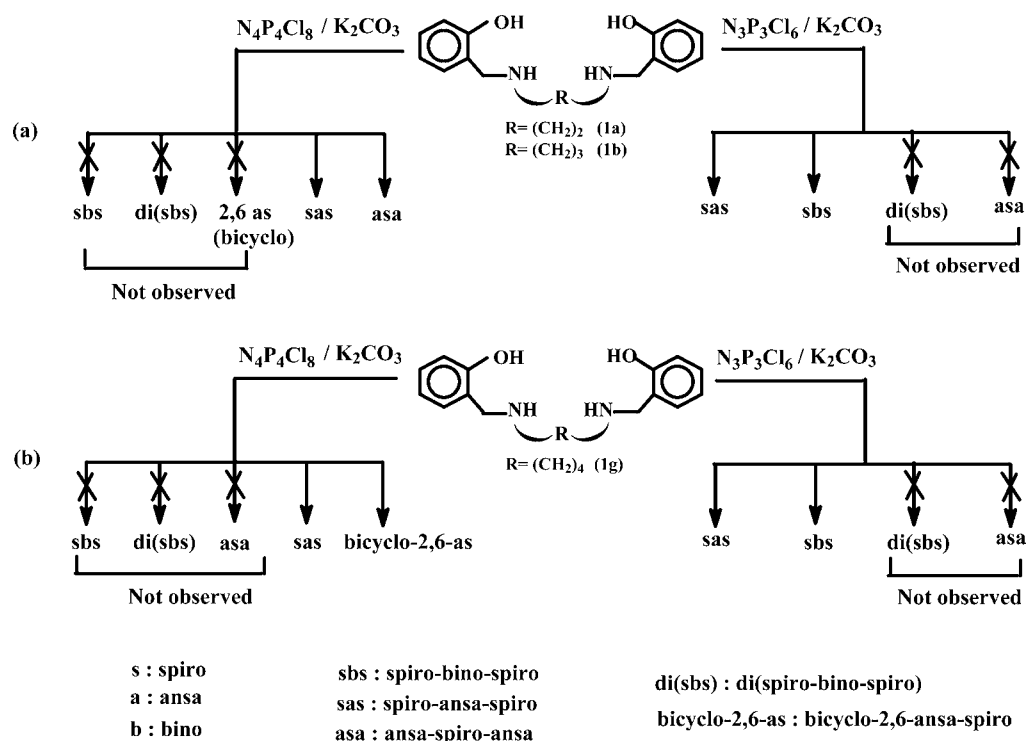


Figure 1. Expected and observed distributions of the reaction products of $N_3P_3Cl_6$ and $N_4P_4Cl_8$ with N_2O_2 donor-type aminopodands.

not observed, whereas for **asa** compounds, the reverse is true. It is noteworthy that the reactions of both $N_3P_3Cl_6$ and $N_4P_4Cl_8$ with these aminopodands (1a and 1b) produce **sas** compounds. Compound 1g, which has the long alkyl chain $(CH_2)_4$, gives **sas** and **sbs** compounds with $N_3P_3Cl_6$, while it produces **sas** (2g) and **bicyclo-2,6-as** (4g) products with $N_4P_4Cl_8$.

The reactions of the partly substituted **sas** (2a and 2b) and **asa** (3a and 3b) phosphazenes with excess pyrrolidine and morpholine in THF produce fully substituted **sas** [(2c and 2d) and (2e and 2f)] and partly substituted *gem*-2-*trans*-6-dichlorophosphazene **asa** [(3c and 3d) and (3e and 3f)] derivatives, respectively (Scheme 1). The complete chloride replacement of 2-*trans*-6-dichlorophosphazene **asa** (3c–3f) compounds with excess pyrrolidine, morpholine, and sodium 4-nitrophenoxide in boiling THF for 6 days was not achieved, indicating that both Cl atoms are significantly inert. The chloride replacement reactions of 3a were carried out separately in THF, toluene, and *o*-xylene by microwave-assisted experiments. The use of microwave irradiation for the preparation of 3c from 3a reduces the reaction time and increases the yield in comparison with the conventional method. Even then, no fully substituted products were obtained; instead, compound 3c was isolated. The microwave-assisted reaction of 3c with excess pyrrolidine did not yield fully substituted products. Consequently, these Cl atoms in **asa** derivatives are highly resistant to replacement reactions by the nucleophile. This may result from both endocyclic P–N bond strengthening and steric hindrance of the bulky N_2O_2 donor-type aminopodands bonded to 2,6-P atoms. The structural data of the **asa** compounds (3a, 3b, and 3e) may support these statements. The values of the P1–N1 and P3–N2 bond lengths are 1.554(1) and 1.561(1) Å for 3a, 1.546(1) and 1.550(1) Å for 3b, and 1.565(1) and 1.561(1) Å for 3e (Table 1). It could be seen that these endocyclic P–N bonds are systematically short, indicating that the electron densities on the P1 and P3 atoms

increase, which can be attributed to the presence of the negative hyperconjugation (see crystallographic part). This situation might be related to the electronic properties of the nonreactive P–Cl bonds. Contemporaneously, the lack of reactivity at P1–Cl1 and P3–Cl2 presumably depends upon the steric effect of the substituents.

The synthetic results mentioned above demonstrate that the choice of the tetradentate symmetric ligands is very important because stereochemically controlled reactions can be achieved. In other words, it is possible to arrange the configurations of tetrahedral P atoms to form controlled stereogenic centers as changing alkyl chain lengths of tetradentate symmetric ligands. All of the compounds have two stereogenic P centers, as discussed later on together with the NMR data of the phosphazene derivatives. The phosphazene derivatives containing N atoms on the spiro or ansa rings have restricted rotation around the P–N and C–N single bonds, leading to atropisomerism, a stereochemical phenomenon^{24a} in which hindered single-bond rotation leads to isolable stereoisomers. Some of the phosphazene derivatives obtained in this study may also have atropisomers.

Data obtained from the microanalyses FTIR, APIES-MS, and 1H , ^{13}C , and ^{31}P NMR, DEPT, HSQC, and HMBC are consistent with the proposed structures of the compounds. The MS spectra of all of the compounds except 2f show the protonated molecular (MH)⁺ ion peaks, while a protonated molecular [M + 2H]⁺ ion peak is observed at *m/z* 808 for 2f. The crystal structures of 2b, 3a, 3b, 3e, and 4g are also determined by X-ray crystallography. To the best of our knowledge, there are no reports on the tetrameric **sas**, **asa**, and **bicyclo-2,6-as** compounds that have been characterized structurally by spectroscopic and/or X-ray diffraction techniques. Spectral and crystallographic data of the compounds are presented in the following.

NMR and IR Spectroscopy. The spin systems of tetrameric phosphazenes indicate that two kinds of novel tetrameric phosphazene derivatives, namely, *sas* (2a–2h) and *asa* (3a–3f), have been prepared, whereas the other expected products such as *sbs* and di(spiro-bino-spiro) [di(*sbs*)] have not been obtained (Figure 1).

As expected, the ^1H -decoupled ^{31}P NMR spectra of *sas* (2a–2h) derivatives exhibit A_2X_2 (A_2B_2 for 2d) type spectra because of two different phosphorus environments within the molecules (Figure 2). The ^1H -decoupled and -coupled ^{31}P NMR spectra

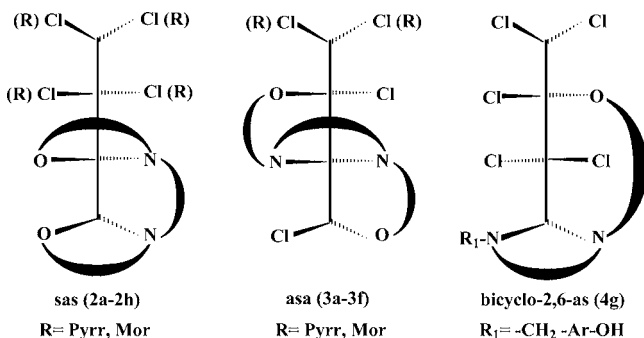


Figure 2. Spatial views of all of the compounds based on the ORTEP diagrams of 2b, 3a, 3b, 3e, and 4g.

of 2a are depicted in Figure S1a,b in the SI, respectively, as examples. One of the multiplets (δ 2.59 ppm) at the ^1H -coupled ^{31}P NMR spectrum is broadened, which indicates the existence of the δ OPN (P_A) P atoms. The δ P and coupling constant ($^2J_{\text{PP}}$) values of the other *sas* derivatives are assigned as 2a (Table 3). The chemical shifts of spiro and PCl_2 values of 2b and 2h are -0.95 and 0.01 and -2.62 and -3.59 ppm, respectively, and the P spiro values are more downfield in contrast to that of 2a, but PCl_2 values are opposite. It is noteworthy that the $^2J_{\text{PP}}$ values for 2a and 2b are considerably lower than the corresponding values in the other *sas* compounds (2c–2f).

The *asa* isomers (3a–3f) having three different phosphorus environments (Figure 2) display the A_2BC (for 3b), ABX_2 (for 3e and 3f), and AB_2X (for 3a, 3c, 3d, and 4g) spin systems consisting of three multiplets at the ^1H -decoupled ^{31}P NMR spectra. As examples, the ^1H -decoupled and -coupled ^{31}P NMR spectra of 3f are depicted in parts a and b of Figure S2 in the SI, respectively. All of the P atoms are unambiguously distinguished from the ^1H -coupled ^{31}P NMR spectrum of 3f, showing three sets of multiplets corresponding to the P spiro (P_A), POCl (P_X), and $\text{P}(\text{mor})_2$ (P_B) groups. The δ P and coupling constant ($^2J_{\text{PP}}$) values of the other *asa* derivatives are also assigned as 3f (Table 3).

Parts a and b of Figure S3 in the SI indicate that the reactions of 1g, K_2CO_3 , and $\text{N}_4\text{P}_4\text{Cl}_8$ produce two kinds of products, *sas* (2g) and bicyclo-2,6-as (4g). Both compounds are separated using column chromatography (Figure S3c,d in the SI). Compound 2g has a A_2X_2 spin system, but the ^{31}P NMR spectrum (AB_2X spin system) of 4g possessing three sets of triplets corresponding to the P spiro (P_A), POCl (P_X), and PCl_2 (P_B) groups is depicted in Figure S3d in the SI. One of the triplets (δ 8.11 ppm) at the ^1H -coupled ^{31}P NMR spectrum is broadened, which indicates the existence of the δ PNN P atom and that the signals of the POCl (δ 5.61 ppm) and PCl_2 groups (δ 4.81 ppm) remain unchanged. The ^1H -decoupled ^{31}P NMR spectrum of 4g shows that the potassium salts of 1g replace

three Cl atoms in $\text{N}_4\text{P}_4\text{Cl}_8$ to give 4g (Figure 2). These results indicate that monopotassium and dipotassium salts of 1g are present in the reaction mixture.

The P atoms of some of the compounds obtained in this study are stereogenic because they have four different substituents. The *sas* phosphazene derivatives (2a–2h) having two equivalent stereogenic P atoms are considered to be only in the meso form because the compounds have symmetric structures. The *asa* phosphazene derivatives (3a–3f), which have trans structures according to Cl atoms, also have two stereogenic P atoms. They are expected to be in the racemic form. However, compound 3b has one enantiomer, as shown by the X-ray structural data, and 3f is a racemic mixture, according to the chiral HPLC and CSA experiments. Compound 4g, having two stereogenic P atoms, is expected to exist as two enantiomers. Table 4 shows stereoisomeric assignments for compounds 2b, 3a, 3b, 3e, 3f, and 4g studied as examples.

Compounds 2a–2h could have racemic and meso forms. However, the only meso forms can form because the compounds have symmetric structures. On the other hand, 4g having two stereogenic P atoms is expected to exist as two enantiomers. According to Table 4, compounds 3a–3f may have racemate (trans) and meso (cis) forms. However, the structure of 3b is crystallized in the noncentrosymmetric space group $P2_12_12_1$, meaning that there is only one enantiomer in the unit cell (Table 1). The Flack absolute structure parameter³² of 3b is refined; the expected values are 0.00 for the correct and +1.00 for the inverted absolute structure. The refined value is 0.03(3). So, the absolute structure (SS) is determined reliably. Because of the presence of the stereogenic centers in all of the phosphazene derivatives, one would expect the occurrence of diastereomers that should give rise to distinguishable NMR signals. Table 3 lists only a single set of signals. The stereogenic properties of the phosphazene derivatives may be determined by ^{31}P NMR spectroscopy in the presence of CSA. The ^{31}P NMR signals of the stereogenic compounds may split into two lines, indicating that they exist as racemates.^{8b} The stereogenic property of 3f is determined by ^{31}P NMR spectroscopy in the presence of CSA using the literature procedure.^{9a,33} As an example, the ^{31}P NMR spectrum of 3f is depicted in Figure 3. In the presence of CSA, the ^{31}P NMR signals of 3f split into two lines (for δ PNN_{mor}), indicating that it exists as a racemate. Upon titration with CSA, the chemical shifts change as a result of the equilibrium between the compound and its ligand-complexed form, and the changes (in ppb) at a mole ratio of CSA–compound of 10:1 are listed in Table 5.

The HPLC method was used for characterization of the racemic (trans) form of 3f. The sample is dissolved in hexane–THF (1:2) at a concentration of $10 \mu\text{g}/\text{mL}$. The separation is made at room temperature. The peak of the solvent front is considered to be equal to the dead time. It is about 2.02 min at a flow rate of 1.5 mL/min. There is resolution of 3f with a separation factor of 1.04 in using a mobile phase containing 96% hexane–4% THF. As expected, there are two peaks for 3f. The peaks for the compound separate into two peaks of the ratio of 1:2 intensity corresponding to the two enantiomers. The peak area of one isomer is 33.1%, and the other one is 66.9%, indicating that both isomers (RR and SS) do not form equally. The HPLC chromatogram of 3f is presented in Figure S4 in the SI. The racemate (3f) in two enantiomers is eluted at 25.993 and 26.925 min. The chromatographic conditions for

Table 3. ^{31}P NMR (Decoupled) Spectral Data of the Compounds^a

R = (CH₂)₂, (CH₂)₃, (CH₂)₄ or (CH₂)₆; Y = Cl, pyr or mor

compound	spin system	OPN	δ (ppm)			$^2J_{\text{PP}}$ (Hz)
			NPN	PCl ₂	POCl	
2a	A ₂ X ₂	2.59		-4.42		$^2J_{\text{AX}} = 16.5$
2b	A ₂ X ₂	-0.95		-2.62		$^2J_{\text{AX}} = 19.5$
2c	A ₂ X ₂	7.08	12.02			$^2J_{\text{AX}} = 33.4$
2d	A ₂ B ₂	4.18	4.46			$^2J_{\text{AB}} = 37.5$
2e	A ₂ X ₂	4.95	7.70			$^2J_{\text{AX}} = 37.2$
2f	A ₂ X ₂	4.37	6.12			$^2J_{\text{AX}} = 39.7$
2g	A ₂ X ₂	6.42		1.76		$^2J_{\text{AX}} = 37.0$
2h	A ₂ X ₂	0.01		-3.59		$^2J_{\text{AX}} = 44.3$
3a	AB ₂ X		12.11	3.44	4.32	$^2J_{\text{AB}} = 49.6$ $^2J_{\text{BX}} = 44.2$
3b	A ₂ BC		-0.31	-1.44	-1.03	$^2J_{\text{AB}} = 56.8$ $^2J_{\text{BC}} = 38.4$
3c	AB ₂ X		12.41 (spiro) 4.24 (pyrr)		6.02	$^2J_{\text{AB}} = 65.0$ $^2J_{\text{BX}} = 51.8$
3d	AB ₂ X		2.53 (spiro) -0.72 (pyrr)		1.14	$^2J_{\text{AB}} = 58.0$ $^2J_{\text{BX}} = 48.1$
3e	ABX ₂		12.33 (spiro) 6.85 (mor)		12.12	$^2J_{\text{AX}} = 42.3$ $^2J_{\text{BX}} = 29.1$
3f	ABX ₂		4.57 (spiro) -0.45 (mor)		1.33	$^2J_{\text{AB}} = 59.9$ $^2J_{\text{BX}} = 55.0$
4g	AB ₂ X		8.11	4.81	5.61	$^2J_{\text{AX}} = 29.1$ $^2J_{\text{BX}} = 28.0$

^aChemical shifts (δ) are reported in ppm and J values in Hz. ^{31}P NMR measurements for **3b** in CD₃CN, for **2c** in toluene, and for other compounds in CDCl₃ solutions at 293 K.

HPLC resolution of trans (**3f**) and the obtained results are presented in Table S1 in the SI. Additionally, this compound is the first example of tetrameric phosphazene derivatives, with chirality confirmed by ^{31}P NMR/CSA and chiral HPLC methods.

The ^1H and ^{13}C NMR signals of both **sas** (**2a–2h**) and **asa** (**3a–3f**) derivatives are assigned on the basis of chemical shifts, multiplicities, coupling constants, and DEPT spectra. The signals of nonprotonated C atoms of **3d** disappear in the DEPT 135 spectrum (Figure S5a in the SI) compared with the ^1H -decoupled ^{13}C NMR spectrum (Figure S5b in the SI). The assignments are made unambiguously by HSQC using values corresponding to $^1J_{\text{CH}}$ and by HMBC using values corresponding to $^2J_{\text{CH}}$, $^3J_{\text{CH}}$, and $^4J_{\text{CH}}$ between the protons and carbons (Table S2 in the SI). The HMBC and HSQC spectra of **3e** are illustrated in Figure S6a,b in the SI, as examples of **asa** (**3a–3f**) phosphazene derivatives. In light of the ^1H and ^{13}C NMR data, **sas** (**2a–2h**) and **asa** (**3a–3f**) compounds seem to have symmetric structures in solution. The X-ray crystallographic data of **2b** confirm its symmetric structure, but **3a**, **3b**, and **3e** do not have symmetric structures in the solid state.

The two bond-coupling constants, $^2J_{\text{PNC}}$, for the NCH₂ carbons of the five-membered spiro rings of **asa** (**3a**, **3c**, and **3e**) compounds are in the ranges of 11.6–12.0 Hz. However, the corresponding values for the **asa** compounds with the six-membered spiro rings (**3b** and **3d**), except **3f** ($^2J_{\text{PNC}} = 4.7$ Hz), are not observed. Furthermore, the $^2J_{\text{PNC}}$ values for NCH₂ carbons of **asa** rings of **sas** (**2a–2f**) derivatives are not also observed. This situation may depend on the size of the rings. The average values of $^3J_{\text{PNC}}$ for the NCH₂CH₂ carbons of **asa** (**3b**, **3d**, and **3f**) derivatives are 8.4 Hz (for spiro rings), 9.6 Hz (for pyrrolidine rings), and 9.4 Hz (for morpholine rings), while the corresponding values of NCH₂CH₂ carbons of **asa** rings for the **sas** compounds are not observed. The δ shifts of aromatic C₁, C₂, C₃, C₄, and C₅ carbons of all of the **asa** (**3a–3f**) compounds are larger than those of the corresponding **sas** (**2a–2f**) derivatives, while the δ shifts of aromatic C₆ carbons are in the opposite direction. In addition, the $^3J_{\text{PNC}}$ values of aromatic C₁ and C₅ carbons of all of the **sas** derivatives are larger than those of the corresponding **asa** derivatives. The average values of C₁ and C₅ carbons are 8.5 and 8.4 Hz for **sas** derivatives and 7.6 and 6.9 Hz for **asa** derivatives, respectively,

Table 4. Theoretical Stereoisomer Distributions and Expected Geometrical Isomers of Compounds 2b, 3a, 3b, 3e, 3f, and 4g

compound	stereogenic P atoms (<i>n</i>)	stereoisomers ^a (2 ^{<i>n</i>}) (expected)		chirality (expected)	chirality (found)	geometrical isomer ^b
2b	2	1	RR	racemic (lines 1/4)	meso (lines 2 = 3)	O1O1 (cis)
		2	RS	meso (lines 2 = 3)		
		3	SR			
		4	SS			
3a, 3e, and 3f	2	1	RR	racemic (lines 1/4)	racemic (lines 1/4)	Cl1Cl2 (trans)
		2	RS	meso (lines 2 = 3)		
		3	SR			
		4	SS			
3b	2	1	RR	racemic (lines 1/4)	enantiomer (line 4)	Cl1Cl2 (trans)
		2	RS	meso (lines 2 = 3)		
		3	SR			
		4	SS			
4g	2	1	RR	enantiomer 1 (lines 1/4)		
		2	RS	enantiomer 2 (lines 2/3)		
		3	SR			
		4	SS			

^aP(OArN) and P(ArOCl) as labeled R/S for 2b, 3a, 3b, 3e, and 3f, respectively, and P(ArOCl) and P(NRN) as labeled R/S for 4g. ^bCis/trans isomerism is labeled explicitly according to Figures 4–8.

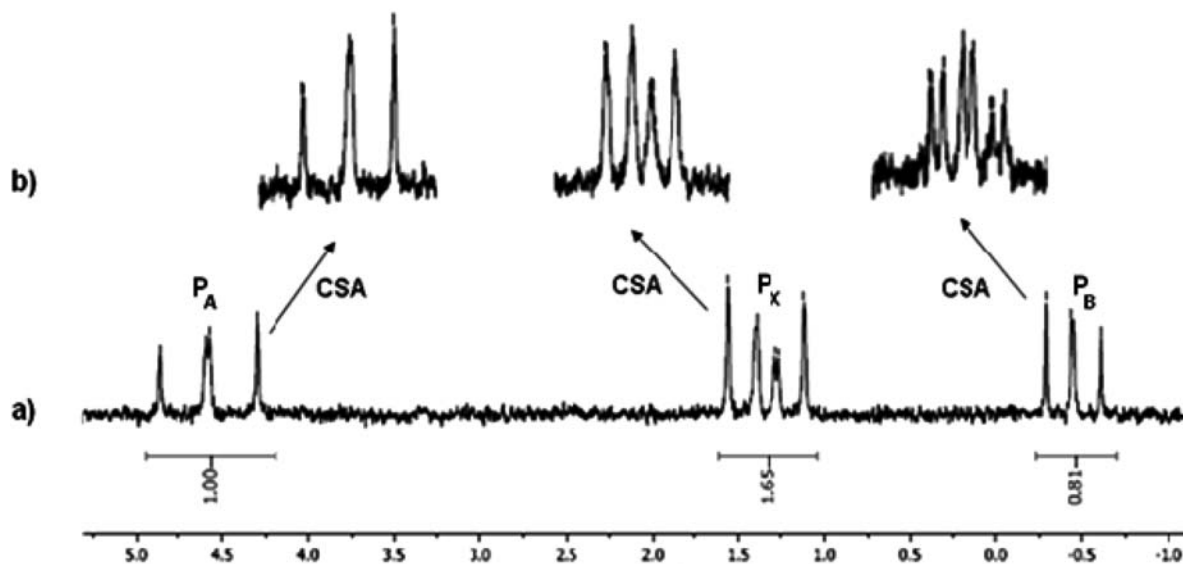


Figure 3. (a) ¹H-decoupled ³¹P NMR spectrum of 3f. (b) Addition of CSA at ca. 10:1 mol ratio showing the doubling of P_B signals, indicating the characteristics of the racemate.

whereas the ²J_{ENC} values of aromatic C₆ carbons are in the reverse direction; e.g., the average values of C₆ carbons are 4.9 Hz [for sas (2a–2f)] and 6.2 Hz [for asa (3a–3f)]. Additionally, the expected 18 carbon signals of 4g are unambiguously assigned from the ¹³C NMR spectrum. The ²J_{ENC} values of benzylic OArCH₂N and C₆ carbons are found to be 6.0, 4.7, and 12.1 Hz, respectively. These values are much larger than those of sas and asa derivatives. The ⁴J_{ENCC} values of aromatic C₂ and C₂' carbons are also found to be 2.1 and 2.2 Hz for 4g.

The ¹H NMR spectra of sas (2c–2f) compounds indicate that four substituents (pyrrolidine or morpholine) are bonded to P atoms, whereas only two substituents (pyrrolidine or morpholine) are bonded to P atoms in asa (3c–3f) derivatives. All of the phosphazene derivatives give very complex ¹H NMR spectra because all of the aliphatic protons are diastereotopic. The diastereotopic benzylic ArCH₂ protons are separated from each other and can be distinguished undoubtedly. One of the

peak groups is in the ranges of δ 4.62–4.32 ppm for sas (2a–2f) and 4.81–4.62 ppm for asa (3a–3f) compounds, whereas the other is in the ranges of δ 4.25–4.01 ppm for sas (2a–2f) and 3.71–3.56 ppm for asa (3a–3f) compounds. As expected, the benzylic protons give rise to an ABX spin system because of the geminal proton–proton coupling and vicinal coupling with the ³¹P nucleus, except 2g, 2h, and 4g. The compounds 2g, 2h, and 4g probably do not exhibit atropisomerism. The large ansa rings (the long alkyl chains in the ansa rings) allow for rotations and lead to enantioconversion at ambient temperatures. Thus, the peaks of benzylic protons are observed as doublets only for 2g, 2h, and 4g. The average ²J_{HH} and ³J_{PH} coupling constants of the compounds sas (2a–2g) and asa (3a–3f) phosphazenes, which have ABX spin systems, are 9.9 and 15.4 Hz and 11.6 and 15.3 Hz, respectively. The δ shift and ³J_{PH} coupling constant of benzylic ArCH₂ of 2h are 4.34 ppm and 14.8 Hz. The benzylic HOArCH₂N and OArCH₂N protons of 4g are observed at 4.32

Table 5. ^{31}P NMR Parameters of Compound **3f** and the Effect of CSA on the ^{31}P NMR Chemical Shifts^a

compound	δ (ppm)		J_{PP} (Hz)
	>P(NN)	>P(OCl)	
(i) ^{31}P NMR Chemical Shifts (ppm) and Geminal PNP Coupling Constants (Hz)			
3f	4.57 (spiro)	1.33	$^2J_{\text{PP}} = 59.9$
	-0.45 (mor)		$^2J_{\text{PP}} = 55.0$
(ii) Effect of CSA on the ^{31}P NMR Chemical Shifts (ppb) at a 10:1 Mole Ratio			
3f	75 (spiro)	22	$^2J_{\text{PP}} = 60.3$
	45 (mor)		$^2J_{\text{PP}} = 54.4$
(iii) Separation of the Enantiomeric Signals (ppb) at a 10:1 Mole Ratio of CSA-Molecule			
3f	<i>b</i> (spiro)	<i>b</i>	
	57 (mor)		

^a ^{31}P NMR measurements in CDCl_3 solutions at 293 K. ^bMagnitude of the effect too small to observe up to a 10:1 mole ratio.

ppm ($^3J_{\text{PH}} = 12.5$ Hz) and 4.24 ppm ($^3J_{\text{PH}} = 8.6$ Hz) as doublets.

The characteristic $\nu_{\text{N-H}}$ bands of aminopodands (**1a**, **1b**, **1g**, and **1h**) at 3276, 3289, 3291, and 3293 cm^{-1} , respectively, are not present in the FTIR spectra of the cyclotetraphosphazenes. The tetrachloro- and pentachlorocyclotetraphosphazenes exhibit strong absorption frequencies in the ranges of 1313–1262 and 1186–1166 cm^{-1} ascribed to $\nu_{\text{P=N}}$ bands of phosphazene rings.³⁴ The asymmetric and symmetric vibration bands of PCl_2 are observed in the ranges of 576–538 and 503–476 cm^{-1} , respectively. The FTIR spectra of the sas (**2a–2f**) and asa (**3a–3f**) phosphazenes exhibit two medium-intensity absorption signals between 3092 and 3057 cm^{-1} and between 3043 and 3019 cm^{-1} attributed to the asymmetric and symmetric stretching vibrations of the Ar–H bonds. Additionally, the $\nu_{\text{O-H}}$ broadening band of **4g** observed at 3327 cm^{-1} indicates hydrogen bonding.

X-ray Structures of 2b, 3a, 3b, 3e, and 4g. The X-ray structural determinations of these compounds confirm the assignments of their structures from spectroscopic data. The molecular and solid-state structures of **2b**, **3a**, **3b**, **3e**, and **4g** along with the atom-numbering schemes are depicted in Figures 4–8, respectively. The asymmetric unit of compound **2b** contains only half a molecule, while the asymmetric units of the remaining compounds contain one crystallographically

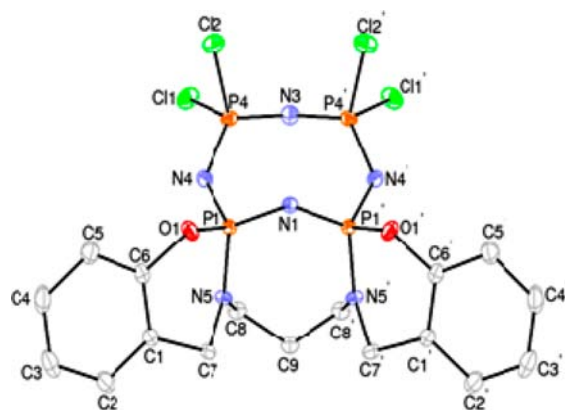


Figure 4. ORTEP-3⁴² drawing of **2b** with the atom-numbering scheme. Displacement ellipsoids are drawn at the 30% probability level.

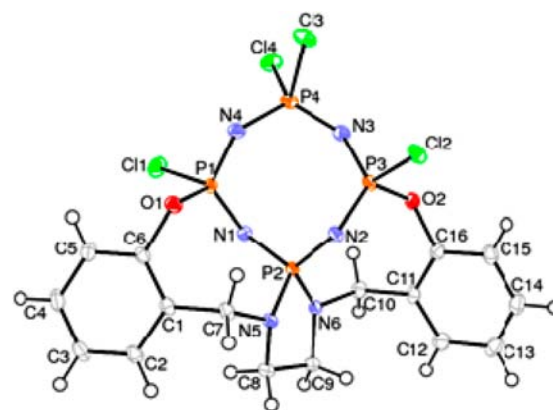


Figure 5. ORTEP-3⁴² drawing of **3a** with the atom-numbering scheme. Displacement ellipsoids are drawn at the 30% probability level.

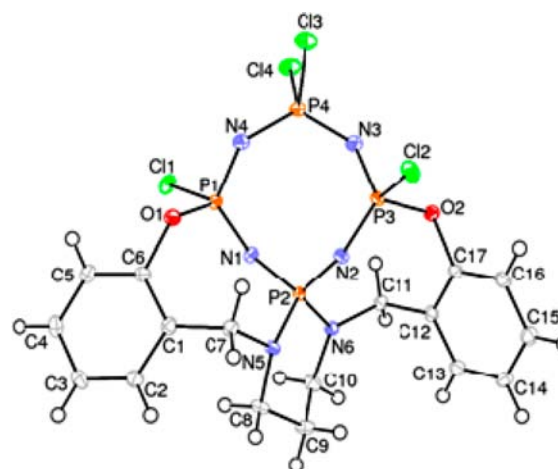


Figure 6. ORTEP-3⁴² drawing of **3b** with the atom-numbering scheme. Displacement ellipsoids are drawn at the 30% probability level.

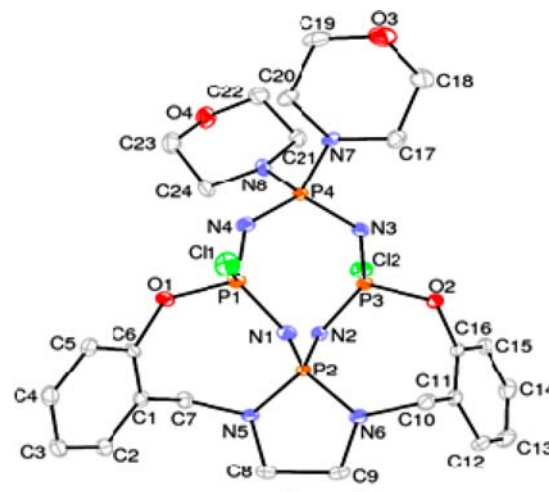


Figure 7. ORTEP-3⁴² drawing of **3e** with the atom-numbering scheme. Displacement ellipsoids are drawn at the 30% probability level.

independent molecule. The four P atoms of **2b**, **3a**, **3b**, **3e**, and **4g** are noncoplanar, and the four N atoms are displaced above (+) and below (–) their best least-squares planes through the P

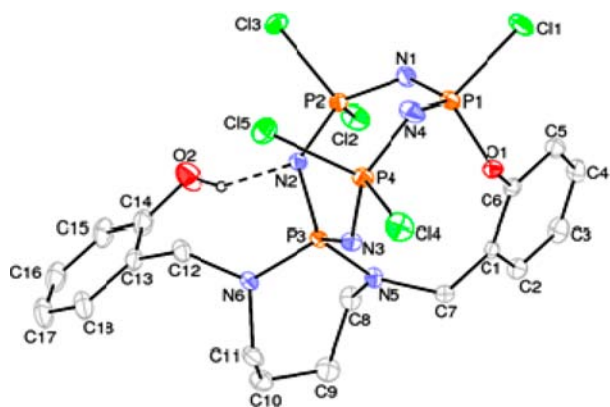


Figure 8. ORTEP-3⁴² drawing of **4g** with the atom-numbering scheme. Displacement ellipsoids are drawn at the 30% probability level. The hydrogen bond is shown as a dashed line.

atoms by the following distances: N1 + 0.0000(1), N3 + 0.0000(1), N4 – 2.0883(1), and N4' + 2.0894(1) for **2b**, N1 + 0.614(1), N2 – 0.667(1), N3 + 0.571(1), and N4 – 0.531(1) for **3a**, N1 – 0.553(1), N2 + 0.554(1), N3 – 0.532(1), and N4 + 0.484(1) for **3b**, N1 + 0.635(2), N2 – 0.639(1), N3 + 0.543(2), N4 – 0.316(2) for **3e** and N1 + 0.090(2), N2 – 0.546(2), N3 + 0.354(2), N4 – 0.375(2) for **4g**. The conformation of the macrocyclic phosphazene rings are depicted by the torsion angles of the ring bonds (Figure S7 in the SI). Compound **2b** consists of a centrosymmetric nonplanar cyclic tetrameric phosphazene ring in a sofa (chair) conformation (Figures S8a in the SI) with the tetradentate ligand (**1b**) bonded to the P atoms in a spiro-ansa-spiro (2,4-sas) fashion, while the crystal structures of **3a**, **3b**, and **3e** indicate that the tetradentate ligands (**1a** and **1b**) are bonded to the P atoms in an ansa-spiro-ansa (2,4,6-asa) fashion and the Cl atoms bonded to the P1 and P3 atoms in a trans fashion. In addition, compound **4g** consists of a bicyclo-2,6-as structure.

In **2b**, the bicyclic part (Figure S8a,b in the SI) is made up of eight-membered tetrameric N₄P₄ and ansa (N1/P1/N5/C8/C9/C8'/N5'/P1') rings fused by a common PNP fragment. The tetrameric N₄P₄ ring is in a sofa conformation, but the ansa ring is in a crown conformation. The six-membered spiro [(P1/O1/C6/C1/C7/N5) and (P1'/O1'/C6'/C1'/C7'/N5')] rings are in twisted-boat conformations [Figure S8c in the SI; Q_T = 2.424(2) Å, φ₂ = 91.17(3)°, and θ₂ = 90.69(8)°]. In **3a**, **3b**, and **3e**, the tricyclic parts (Figures S9b, S10b, and S11b in the SI) are made up of three eight-membered rings, which are not planar, having total puckering amplitudes, Q_T,³⁵ of 1.206(1) Å (for the tetrameric N₄P₄ ring of **3a**), 1.379(4) Å [for the ansa (P1/N1/P2/N5/C7/C1/C6/O1) ring of **3a**], 3.607(2) Å [for the ansa (P3/N2/P2/N6/C10/C11/C16/O2) ring of **3a**], 1.088(1) Å [for the tetrameric N₄P₄ ring of **3b**], 1.073(2) Å [for the ansa (P1/N1/P2/N5/C7/C1/C6/O1) ring of **3b**], 3.644(2) Å (for the ansa (P3/N2/P2/N6/C11/C12/C17/O2) ring of **3b**], 1.089(1) Å (for the tetrameric N₄P₄ ring of **3e**), 1.352(2) Å [for the ansa (P1/N1/P2/N5/C7/C1/C6/O1) ring of **3e**], and 2.756(4) Å (for the ansa (P3/N2/P2/N6/C10/C11/C16/O2) ring of **3e**). In **3a** and **3e**, the five-membered spiro rings (P2/N5/C8/C9/N6) are in twisted conformations (Figure S9c in the SI for **3a** and Figure S11c in the SI for **3e**). In **3b**, the six-membered spiro ring is in a chair conformation [Figure S10c in the SI; Q_T = 0.749(5) Å, φ₂ = –21.1(1)°, and θ₂ = 140.2(1)°]. In **4g**, the bicyclic system made up of phosphazene and the ansa (P1/N4/P4/N3/P3/

N5/C7/C1/C6/O1) rings is not planar, having total puckering amplitudes, Q_T,³⁵ of 1.187(1) Å (for the tetrameric N₄P₄ ring) and 1.509(1) Å (for the ansa ring) [Figure S12a,b in the SI]. The seven-membered ring (P3/N5/C8/C9/C10/C11/N6) has a twisted conformation with a total puckering amplitude, Q_T, of 1.317(3) Å (Figure S12c in the SI).

In the phosphazene rings, the endocyclic P–N bond lengths are in the ranges of 1.560(1)–1.594(1) Å (for **2b**), 1.554(1)–1.603(1) Å (for **3a**), 1.546(1)–1.610(1) Å (for **3b**), 1.549(2)–1.605(2) Å (for **3e**), and 1.544(2)–1.640(2) Å (for **4g**) (Table 2). The average endocyclic P–N bond lengths in tetrameric phosphazene rings are 1.573(1), 1.576(1), 1.573(1), 1.576(2), and 1.575(1) Å, which are shorter than the average exocyclic P–N bond lengths of 1.614(1), 1.645(1), 1.641(1), 1.644(2), and 1.624(2) Å for **2b**, **3a**, **3b**, **3e**, and **4g**, respectively. In phosphazenes, the P–N single and double bonds are generally in the ranges of 1.628–1.691 and 1.571–1.604 Å, respectively,³⁶ and they are among the most intriguing bonds in phosphazene chemistry. Recently, natural bond orbital (NBO) and topological electron density analyses are used to investigate the electronic structures of phosphazenes.³⁷ The most likely phosphazene bonding alternatives, namely, negative hyperconjugation and ionic bonding, were evaluated using NBO. Ionic bonding was found to be the dominant feature, and the multiple-bond character could be attributed, in part, to the presence of negative hyperconjugation.^{4e,38}

As can be seen from Table 2, the P–N–P bond angles of **2b**, **3a**, **3b**, **3e**, and **4g** are in the ranges of 126.91(10)–141.37(14)°, 128.27(8)–129.35(7)°, 129.52(10)–134.27(9)°, 128.15(10)–137.42(10)°, and 127.01(11)–133.64(12)° [the average value is 131.0(1)°]. The P–N–P bond angles of **3a** are almost the same, but the others are spread. In the literature,^{4b,39} similar spreads of P–N–P angles were found in some phosphazene derivatives. The variations in the endocyclic N–P–N bond angles are also very large, ranging from 114.00(9)° to 122.57(10)° (for **2b**), from 112.89(6)° to 123.31(6)° (for **3a**), from 112.44(7)° to 123.71(7)° (for **3b**), from 113.09(8)° to 125.27(8)° (for **3e**), and from 113.94(9)° to 123.00(11)° (for **4g**) with an average value of 119.82(8)°. The endocyclic N–P–N bond angles (for P atoms containing spiro substituents) are much affected by the N₂O₂ donor-type tetradentate ligands (**1a**–**1d**) bonded to the P atoms [average value is 113.27(8)°], while the exocyclic N–P–N bond angles are less affected compared to the corresponding angle in the standard compound, N₄P₄Cl₈. In N₄P₄Cl₈, the endocyclic N–P–N and P–N–P and exocyclic Cl–P–Cl bond angles are 121.2°, 131.3°, and 102.8°. The variations of the P–N–P and N–P–N angles of **2b**, **3a**, **3b**, **3e**, and **4g** may reflect the steric hindrances of the bulky side groups and could be ascribed to the substituent-dependent charges at the P centers and negative hyperconjugation.^{4e,37,38}

Moreover, compound **4g** consists of a bicyclo-2,6-as structure with an intramolecular O2–H2A···N2 hydrogen bond (Figure 8).⁴¹ The C–H···π contacts in compounds **3a**, **3b**, and **3e** may further stabilize the structure (Table S3 in the SI).

Antimicrobial Activities. The tetrapyrrolidinocyclotetraphosphazene derivatives (**2c** and **2d**) exhibit weak antibacterial activity against (G+) bacterium, and racemic *gem*-2-*trans*-6-dichloropyrrolidinocyclotetraphosphazene derivatives (**3c** and **3d**) show moderate antifungal activity against only *Candida tropicalis*. The starting compound (N₄P₄Cl₈), pyrrolidine, morpholine, **1a**, **1b**, **1g**, and **1h** are checked for the same

bacteria and fungi. Morpholine and $N_4P_4Cl_8$ exhibit weak antibacterial activity against *Pseudomonas aeruginosa* (G⁻), **1b**, and $N_4P_4Cl_8$ to *Bacillus cereus* (G⁺), **1b**, to *Escherichia coli* (G⁻), **1h**, to *Staphylococcus aureus* (G⁺), **1g**, to *Bacillus subtilis* (G⁺). None of them shows antifungal activity. The results are given in section S1 in the SI for comparison to the cyclotetraphosphazene derivatives. The antifungal activity of **3c** and **3d** may have arisen from the whole structure of these compounds.

Interaction with pBR322 Plasmid DNA and Restriction Enzyme Digestion. Interactions of the starting compound ($N_4P_4Cl_8$), pyrrolidine, morpholine, **1a**, **1b**, **1g**, and **1h** and cyclotetraphosphazene derivatives **2a–2f** and **3a–3f** with supercoiled pBR322 DNA were investigated using agarose gel electrophoresis. Pyrrolidine, morpholine, **1a**, **1b**, **1g**, and **1h** have no effect on plasmid DNA except $N_4P_4Cl_8$. However, it was observed that compounds **2e**, **3c**, and **3e** are able to cleave the DNA. The presence of the linear form III in the DNA–compound mixtures indicates the conformational changes of DNA. It is noteworthy that the covalent interactions may play an important role in the changes. Moreover, restriction analyses indicate that **2a–2f** and **3a–3f** compounds bind to GG of the DNA except compound **2b** and partly **2e** (section S2 in the SI).

CONCLUSIONS

In summary, the reactions of $N_4P_4Cl_8$ with the N_2O_2 donor-type tetradentate ligands (**1a**, **1b**, **1g**, and **1h**) give two kinds of novel *sas* (**2a**, **2b**, **2g**, and **2h**) and *asa* (**3a** and **3b**) tetraphosphazene derivatives, which are the first examples of multiheterocyclic cyclotetraphosphazenes. The partly substituted *sas* (**2a** and **2b**) compounds reacted with excess pyrrolidine and morpholine in THF to produce tetrapyrrolidinocyclotetraphosphazenes (**2c** and **2d**) and tetramorpholinocyclotetraphosphazenes (**2e** and **2f**). The reactions of partly substituted *asa* (**3a** and **3b**) derivatives with excess pyrrolidine and morpholine in THF produce partly substituted *gem-2-trans-6-dichloropyrrolidinocyclotetraphosphazenes* (**3c** and **3d**) and *-morpholinocyclotetraphosphazenes* (**3e** and **3f**). The partly substituted phosphazenes could be useful as precursors for preparing unique mixed-substituent phosphazenes because the chiral systems and biologically active materials exhibit chemotherapeutic or antibacterial activity behaviors. The fully substituted phosphazenes (**2c–2f**) are possible ligating agents for transition-metal cations. All of the compounds were fully characterized by one- and two-dimensional NMR techniques, where the compounds (**2b**, **3a**, **3b**, **3e**, and **4g**) have been characterized crystallographically. From the NMR and X-ray crystallographic results, it was shown that the stereogenic P and N centers are likely to be generated using tetradentate symmetric ligands. Moreover, atropisomerism may arise from the restricted single-bond rotations about N atoms. The investigations of the possible stable conformers of atropisomers are an important topic for future research in our group. In **2a–2h**, which are symmetric structures, there are two stereogenic P atoms and they are in meso form, while the interesting compound **4g**, which is accidentally obtained from the reaction of $N_4P_4Cl_8$ with **1g**, has two stereogenic P atoms and is expected to be in enantiomeric mixtures. On the other hand, in **3a–3f**, there are also two stereogenic P atoms. X-ray crystallographic data confirm that **3b** has one enantiomer (SS). Additionally, the stereogenic property of **3f** was determined by ^{31}P NMR spectroscopy in the presence of CSA and chiral HPLC methods.

Further detailed studies of the long-chain aminopodands with $N_4P_4Cl_8$ are under investigation.

ASSOCIATED CONTENT

Supporting Information

Additional figures giving 1H -decoupled and 1H -coupled ^{31}P NMR spectra of **2b**, **3f**, and **4g** (Figures S1–S3), HPLC profile of compound **3f** (Figure S4), the DEPT and ^{13}C NMR spectra of **3d** (Figure S5), the HMBC and HSQC spectra of **3e** (Figure S6), the shape of the phosphazene rings in **2b**, **4g**, **3a**, **3b**, and **3e** with torsion angles given (Figure S7), crystal ring conformations (Figures S8–S12), X-ray crystallographic files in CIF format for compounds **2b**, **3a**, **3b**, **3e**, and **4g**, chromatographic conditions for TLC and HPLC resolution of racemic cyclotetraphosphazene derivative (**3f**) (Table S1), 2D 1H – ^{13}C HSQC and HMBC correlations for compounds **2a**, **2b**, **2c**, **3a**, **3c**, and **3e** (Table S2), hydrogen-bond geometries (Table S3), antimicrobial activities (section S1), and DNA and compound interactions (section S2). This material is available free of charge via the Internet at <http://pubs.acs.org>.

AUTHOR INFORMATION

Corresponding Author

*E-mail: zkilic@science.ankara.edu.tr

Notes

The authors declare no competing financial interest.

ACKNOWLEDGMENTS

The authors thank the Scientific and Technical Research Council of Turkey (Grant 211T019) and the Medicinal Plants and Medicine Research Center of Anadolu University, Eskişehir, for use of their X-ray and NMR facilities. T.H. is indebted to Hacettepe University, Scientific Research Unit (Grant 0202602002), for their financial support. L.A. grateful to State Planning Organisation for financial support for the research (Grant No. 1998K121480). The authors acknowledge Professor C. Allen for his helpful scientific discussions and corrections.

REFERENCES

- (1) (a) Chandrasekhar, V.; Thilagar, P.; Pandian, B. M. *Coord. Chem. Rev.* **2007**, *251*, 1045–1074. (b) Allen, C. W. *Chem. Rev.* **1991**, *91*, 119–135. (c) Schmutz, J. L.; Allcock, H. R. *Inorg. Chem.* **1975**, *14*, 2433–2438. (d) Labarre, J. F. *Top. Curr. Chem.* **1985**, *129*, 173–230.
- (2) (a) Myer, C. N.; Allen, W. C. *Inorg. Chem.* **2002**, *41*, 60–66. (b) Jung, J. H.; Potluri, S. K.; Zhang, H.; Neilson, P. W. *Inorg. Chem.* **2004**, *43*, 7784–7791. (c) Keshav, K.; Singh, N.; Elias, A. J. *Inorg. Chem.* **2010**, *49*, 5753–5765. (d) Kılıç, Z.; Okumuş, A.; Demiriz, Ş.; Bilge, S.; Öztürk, A.; Hökelek, T. *J. Incl. Phenom. Macrocycl. Chem.* **2009**, *65*, 269–286. (e) Yenilmez, Ç. G.; Tanrıverdi, E.; Zorlu, Y. *Heterocycles* **2008**, *75* (3), 635–643. (f) İbişoğlu, H. *Heterocycles* **2007**, *71* (10), 2173–2181. (g) Okumuş, A.; Bilge, S.; Kılıç, Z.; Öztürk, A.; Hökelek, T.; Yılmaz, F. *Spectrochim. Acta, Part A* **2010**, *76*, 401–409. (h) Deutch, W. F.; Hursthouse, M. B.; Kılıç, Z.; Parkers, H. G.; Shaw (nee Gözen), L. S.; Shaw, R. A. *Phosphorus, Sulfur, Silicon* **1987**, *32*, 81–85. (i) Özen, F.; Çil, E.; Arslan, M. J. *Chem. Soc. Pak.* **2012**, *34* (3), 690–698. (j) Işıklan, M.; Sonkaya, Ö.; Çoşut, B.; Yeşilot, S.; Hökelek, T. *Polyhedron* **2010**, *29*, 1612–1618. (k) Çil, E.; Tanyıldızı, M. A.; Özen, F.; Boybay, M.; Arslan, M.; Görgülü, A. O. *Arch. Pharm. Chem. Life Sci.* **2012**, *345*, 476–485.
- (3) (a) Brandt, K.; Bartczak, T. J.; Kruszynski, R.; Porwollik-Czomperlik, I. *Inorg. Chim. Acta* **2001**, *322*, 138–144. (b) Porwollik-Czomperlik, I.; Siwy, M.; Şek, D.; Kaczmarczyk, B.; Nasulewicz, A.; Jaroszewicz, I.; Pelczynska, M.; Opolski, A. *Acta Pol. Pharm.* **2004**, *66*,

- 267–272. (c) Andrews, R. *IRCS Med. Sci.* **1979**, *7*, 285. (d) Guerch, G.; Labarre, J. F.; Lahana, R.; Roques, R.; Sournie, F. *J. Mol. Struct.* **1983**, *99*, 275–282.
- (4) (a) Contractor, S. R.; Kılıç, Z.; Shaw, R. A. *J. Chem. Soc., Dalton Trans.* **1987**, 2023–2029. (b) Işıklan, M.; Kılıç, Z.; Akduran, N.; Hökelek, T. *J. Mol. Struct.* **2003**, *660*, 167–179. (c) Bešli, S.; İbişoğlu, H.; Kılıç, A.; Ün, İ.; Yüksel, F. *Polyhedron* **2010**, *29*, 3220–3228. (d) Alkubaisi, A. H.; Shaw, R. A. *Phosphorus, Sulfur, Silicon* **1989**, *45*, 7–14. (e) Ainscough, E. W.; Brodie, A. M.; Chaplin, A. B.; Derwahl, A.; Harrison, J. A.; Otter, C. A. *Inorg. Chem.* **2007**, *46*, 2575–2583. (f) Kumaraswamy, S.; Vijjulatha, M.; Muthiah, C.; Kumara Swamy, K. C.; Engelhardt, U. *J. Chem. Soc., Dalton Trans.* **1999**, 891–899. (g) Yıldız, M.; Kılıç, Z.; Hökelek, T. *J. Mol. Struct.* **1999**, *510*, 227–235. (h) Liu, X.; Breon, J. P.; Chen, C.; Allcock, H. R. *Dalton Trans.* **2012**, *41*, 2100–2109. (i) Kumar, D.; Singh, N.; Keshav, K.; Elias, A. J. *Inorg. Chem.* **2011**, *50*, 250–260.
- (5) (a) İbişoğlu, H.; Yenilmez, Ç. G.; Kılıç, A.; Tanrıverdi, E.; Ün, İ.; Dal, H.; Hökelek, T. *J. Chem. Sci.* **2009**, *121*, 125–135. (b) Cameron, T. S.; Linden, A.; Guerch, G.; Bonnet, J. P.; Labarre, J. *J. Mol. Struct.* **1989**, *212*, 295–304. (c) Kılıç, A.; Kılıç, Z.; Shaw, R. A. *Phosphorus, Sulfur, Silicon* **1991**, *57*, 111–117.
- (6) (a) Chandrasekhar, V.; Karthikeyan, S.; Krishnamurthy, S. S.; Woods, M. *Indian J. Chem.* **1985**, *24A*, 379–383. (b) Chandrasekhar, V.; Krishnan, V. *Adv. Inorg. Chem.* **2002**, *53*, 159–211. (c) Allcock, H. R.; Diefenbach, U.; Pucher, S. R. *Inorg. Chem.* **1994**, *33*, 3091–3095.
- (7) (a) Bilge, S.; Demiriz, Ş.; Okumuş, A.; Kılıç, Z.; Tercan, B.; Hökelek, T.; Büyükgüngör, O. *Inorg. Chem.* **2006**, *45*, 8755–8767. (b) Safran, S.; Hökelek, T.; Bilge, S.; Demiriz, Ş.; Natsagdorj, A.; Kılıç, Z. *Anal. Sci.* **2005**, *21*, 77–78. (c) Tercan, B.; Hökelek, T.; Bilge, S.; Natsagdorj, A.; Demiriz, Ş.; Kılıç, Z. *Acta Crystallogr.* **2004**, *E60*, 795–797.
- (8) (a) Bešli, S.; Coles, S. J.; Davies, D. B.; Eaton, R. J.; Hursthouse, M. B.; Kılıç, A.; Shaw, R. A.; Çiftçi, G. Y.; Yeşilot, S. *J. Am. Chem. Soc.* **2003**, *125*, 4943–4950. (b) Işıklan, M.; Asmafiliz, N.; Özalp, E. E.; İlter, E. E.; Kılıç, Z.; Çoşut, B.; Yeşilot, S.; Kılıç, A.; Öztürk, A.; Hökelek, T.; Koç, L. Y.; Açıık, L.; Akyüz, E. *Inorg. Chem.* **2010**, *49*, 7057–7071. (c) Coles, S. J.; Davies, D. B.; Eaton, R. J.; Hursthouse, M. B.; Kılıç, A.; Mayer, T. A.; Shaw, R. A.; Yenilmez, G. *J. Chem. Soc., Dalton Trans.* **2002**, 365–370. (d) İlter, E. E.; Asmafiliz, N.; Kılıç, Z.; Işıklan, M.; Hökelek, T.; Çaylak, N.; Şahin, E. *Inorg. Chem.* **2007**, *46*, 9931–9944. (e) Ün, Ş. Ş.; Uslu, A.; Yeşilot, S.; Ün, İ.; Çoşut, B.; Yüksel, F.; Kılıç, A. *Polyhedron* **2011**, *30*, 1587–1594.
- (9) (a) Asmafiliz, N.; Kılıç, Z.; Öztürk, A.; Hökelek, T.; Koç, L. Y.; Açıık, L.; Kısa, Ö.; Albay, A.; Üstündağ, Z.; Solak, A. O. *Inorg. Chem.* **2009**, *48*, 10102–10116. (b) Alvarez, J. L. G.; Amato, M. E.; Lombardo, G. M.; Carriedo, G. A.; Punzo, F. *Eur. J. Inorg. Chem.* **2010**, 28, 4483–4491. (c) Çoşut, B.; İbişoğlu, H.; Kılıç, A.; Yeşilot, S. *Inorg. Chim. Acta* **2009**, *362*, 4931–4936. (d) Yeşilot, S.; Çoşut, B. *Inorg. Chem. Commun.* **2007**, *10*, 88–93. (e) Bešli, S.; Davies, D. B.; Kılıç, A.; Shaw, R. A.; Şahin, Ş.; Uslu, A.; Yeşilot, S. *J. Chromatogr. A* **2006**, *1132*, 201–205.
- (10) (a) Ainscough, E. W.; Brodie, A. M.; Davidson, R. J.; Otter, C. A. *Inorg. Chem. Commun.* **2008**, *11*, 171–174. (b) Gleria, M.; Jaeger, R. D. *Applicative Aspects of Cyclophosphazenes*; Nova Science Publishers, Inc.: Hauppauge, NY, 2004. (c) Çoşut, B.; Durmuş, M.; Kılıç, A.; Yeşilot, S. *Inorg. Chim. Acta* **2011**, *366*, 161–172. (d) Ainscough, E. W.; Brodie, A. M.; Davidson, R. J.; Moubaraki, B.; Murray, K. S.; Otter, C. A.; Waterland, M. R. *Inorg. Chem.* **2008**, *47* (20), 9182–9192.
- (11) (a) Allcock, H. R.; Napierala, M. E.; Cameron, C. G.; O'Connor, S. J. M. *Macromolecules* **1996**, *29*, 1951–1956. (b) Liu, J.; Tang, J.; Wang, X.; Wu, D. *RSC Adv.* **2012**, *2*, 5789–5799.
- (12) Singler, R. E.; Deome, A. J.; Dunn, D. A.; Bieberich, M. J. *Ind. Eng. Chem. Prod. Res. Dev.* **1986**, *25* (1), 46–57.
- (13) Zhu, J.; Liu, W.; Chu, R.; Meng, X. *Tribol. Int.* **2007**, *40* (1), 10–14.
- (14) Omotowa, B. A.; Phillips, B. S.; Zabinski, J. S.; Shreeve, J. M. *Inorg. Chem.* **2004**, *43*, 5466–5471.
- (15) (a) Allcock, H. R.; Klingenberg, E. H. *Mater. Sci.: Crystallogr.* **1995**, *28*, 4351–4360. (b) Allcock, H. R.; Kim, C. *Macromolecules* **1991**, *24*, 2846–2851.
- (16) Allcock, H. R. *Curr. Opin. Solid State Mater. Sci.* **2006**, *10*, 231–240.
- (17) (a) Xu, G.; Lu, Q.; Yu, B.; Wen, L. *Solid State Ionics* **2006**, *177*, 305–309. (b) Morford, R. V.; Kellam, E. C.; Hofmann, M. A.; Baldwin, R.; Allcock, H. R. *Solid State Ionics* **2000**, *133*, 171–177. (c) Allcock, H. R.; Kellam, E. C.; Morford, R. V.; Conner, D. A.; Welna, D. T.; Chang, Y.; Allcock, H. R. *Macromolecules* **2007**, *40*, 322–328. (d) Klein, R.; Welna, D. T.; Weikel, A.; Allcock, H. R.; Runt, J. *Macromolecules* **2007**, *40*, 3990–3995. (e) Harrup, M. K.; Gering, K. L.; Rollins, H. W.; Sazhin, S. V.; Benson, M. T.; Jamison, D. K.; Michelbacher, C. J.; Luther, T. A. *ESC Trans.* **2012**, *41* (39), 13–25.
- (18) (a) Siwy, M.; Şek, D.; Kaczmarczyk, B.; Jaroszewicz, I.; Nasulewicz, A.; Pelczynska, M.; Nevozhay, D.; Opolski, A. *J. Med. Chem.* **2006**, *49*, 806–810. (b) İlter, E. E.; Asmafiliz, N.; Kılıç, Z.; Açıık, L.; Yavuz, M.; Bali, E. B.; Solak, A. O.; Büyükkaya, F.; Dal, H.; Hökelek, T. *Polyhedron* **2010**, *29*, 2933–2944.
- (19) Singh, A.; Krogman, N. R.; Sethurman, S.; Nair, L. S.; Sturgeon, J. L.; Brown, P. W.; Laurencin, C. T.; Allcock, H. R. *Biomacromolecules* **2006**, *7*, 914–918.
- (20) Greish, Y. E.; Bender, J. D.; Lakshmi, S.; Brown, P. W.; Allcock, H. R.; Laurencin, C. T. *Biomaterials* **2005**, *26*, 1–9.
- (21) Nair, L.; Bhattacharyya, S.; Bender, J. D.; Greish, Y. E.; Brown, P. W.; Allcock, H.; Laurencin, C. T. *Biomacromolecules* **2004**, *5*, 2212–2220.
- (22) Bovin, J. O.; Galy, J.; Labarre, J. F.; Sournie, F. *J. Mol. Struct.* **1978**, *49* (2), 421–423.
- (23) Zhu, X.; Liang, Y.; Zhang, D.; Wang, L.; Ye, Y.; Zhao, Y. *Phosphorus, Sulfur, Silicon Relat. Elem.* **2011**, *186*, 281–286.
- (24) (a) He, L.; Chen, X. H.; Wang, D. N.; Luo, S. W.; Zhang, W. Q.; Yu, J.; Ren, L.; Gong, L. Z. *J. Am. Chem. Soc.* **2011**, *133* (34), 13504–13518. (b) Bishwajit, P.; Butterfoss, G. L.; Boswell, M. G.; Renfrew, P. D.; Yeung, F. G.; Shah, N. H.; Wolf, C.; Bonneau, R.; Kirshenbaum, K. *J. Am. Chem. Soc.* **2011**, *133*, 10910–10919.
- (25) Bruker program 1D WIN-NMR (release 6.0) and 2D WIN-NMR (release 6.1).
- (26) Perez, C.; Paul, M.; Bazerque, P. *Acta Biol. Med. Exp.* **1990**, *15*, 113–115.
- (27) Gümüş, F.; Eren, G.; Açıık, L.; Çelebi, A.; Öztürk, F.; Yılmaz, S.; Sakan, R.; Gür, S.; Özkul, A.; Elmali, A.; Elerman, Y. *J. Med. Chem.* **2009**, *52*, 1345–1357.
- (28) Fritsch, J.; Sambrook, T.; Maniatis, T. *Molecular Cloning*; Cold Spring Harbor Laboratory Press: New York, 1989.
- (29) (a) Bilge, S.; Natsagdorj, A.; Demiriz, Ş.; Çaylak, N.; Kılıç, Z.; Hökelek, T. *Helv. Chim. Acta* **2004**, *87*, 2088–2099. (b) Ghose, B. N.; Lasisi, K. M. *Synt. React. Inorg. Met.-Org. Chem.* **1986**, *16*, 1121–1133. (c) Signorini, O.; Dockal, E. R.; Castellano, G.; Oliva, G. *Polyhedron* **1996**, *15*, 245–255. (d) Bilge, S.; Natsagdorj, A.; Akduran, N.; Hökelek, T.; Kılıç, Z. *J. Mol. Struct.* **2002**, *611*, 169–178. (e) Panova, G. V.; Potapov, V. M.; Turovets, I. M.; Golub, E. G. *Zh. Obshch. Khim.* **1983**, *53*, 1612–1620. (f) Hökelek, T.; Akduran, N.; Bilge, S.; Kılıç, Z. *Anal. Sci.* **2001**, *17*, 801–802. (g) Hökelek, T.; Bilge, S.; Kılıç, Z. *Acta Crystallogr., Sect. E* **2003**, *59*, 1607–1609. (h) Atwood, D. A.; Benson, J.; Jegier, J. A.; Lindholm, N. F.; Martin, K. J.; Pitura, R. J.; Rutherford, D. *Main Group Chem.* **1995**, *1* (1), 99–113.
- (30) SADABS; Bruker AXS Inc.: Madison, WI, 2005.
- (31) Sheldrick, G. M. *Acta Crystallogr., Sect. A* **2008**, *64*, 112–122.
- (32) Flack, H. D. *Acta Crystallogr.* **1983**, *A39*, 876–881.
- (33) (a) Bešli, S.; Coles, S. J.; Davies, D. B.; Eaton, R. J.; Hursthouse, M. B.; Kılıç, A.; Shaw, R. A.; Uslu, A.; Yeşilot, S. *Inorg. Chem. Commun.* **2004**, *7*, 842–846. (b) Coles, S. J.; Davies, D. B.; Hursthouse, M. B.; Kılıç, A.; Şahin, Ş.; Shaw, R. A.; Uslu, A. *J. Organomet. Chem.* **2007**, *692*, 2811–2821. (c) Coles, S. J.; Davies, D. B.; Eaton, R. J.; Hursthouse, M. B.; Kılıç, A.; Shaw, R. A.; Uslu, A. *Dalton Trans.* **2006**, *10*, 1302–1312. (d) Uslu, A. *Inorg. Chem. Commun.* **2005**, *8*, 1002–1008.

(34) (a) Carriedo, G. A.; Alonso, F. G.; Gonzalez, P. A.; Menendez, J. *R. J. Raman Spectrosc.* **1998**, *29*, 327–330. (b) Okumuş, A.; Kılıç, Z.; Hökelek, T.; Dal, H.; Açıık, L.; Öner, Y.; Koç, L. Y. *Polyhedron* **2011**, *30*, 2896–2907.

(35) Cremer, D.; Pople, J. A. *J. Am. Chem. Soc.* **1975**, *97* (6), 1354–1358.

(36) Allen, F. H.; Kennard, O.; Watson, D. G.; Brammer, L.; Orpen, G.; Taylor, R. *J. Chem. Soc., Perkin Trans. 2* **1987**, *12*, 1–19.

(37) Chaplin, A. B.; Harrison, J. A.; Dyson, P. J. *Inorg. Chem.* **2005**, *44*, 8407–8417.

(38) (a) Krishnamurthy, S. S. *Phosphorus, Sulfur, Silicon Relat. Elem.* **1994**, *87*, 101–111. (b) Davidson, R. J.; Ainscough, E. W.; Brodie, A. M.; Harrison, J. A.; Waterland, M. R. *Eur. J. Inorg. Chem.* **2010**, 1619–1625.

(39) (a) Hökelek, T.; Kılıç, A.; Begeç, S.; Yıldız, M. *Acta Crystallogr.* **1996**, *C52*, 3243–3246. (b) Hökelek, T.; Kılıç, E.; Kılıç, Z. *Acta Crystallogr.* **1998**, *C54*, 1295–1297. (c) Hökelek, T.; Kılıç, E.; Kılıç, Z. *Acta Crystallogr.* **1999**, *C55*, 983–985.

(40) Wagner, A. J.; Vos, A. *Acta Crystallogr.* **1968**, *B24*, 707–713.

(41) Bilge, S.; Kılıç, Z.; Hayvalı, Z.; Hökelek, T.; Safran, S. *J. Chem. Sci.* **2009**, *121* (6), 989–1001.

(42) Farrugia, L. J. *J. Appl. Crystallogr.* **1997**, *30*, 565–566.